Cretaceous Research 37 (2012) 100–126

Contents lists available at SciVerse ScienceDirect

Cretaceous Research

journal homepage: www.elsevier.com/locate/CretRes

Planktonic foraminiferal and calcareous nannofossil biostratigraphy and magnetostratigraphy of the uppermost Campanian and Maastrichtian at Zumaia, northern Spain

Irene Pérez-Rodríguez [a,*], Jacqueline A. Lees [b], Juan C. Larrasoaña [c], José A. Arz [a], Ignacio Arenillas [a]

[a] Departamento de Ciencias de la Tierra (Paleontología) e Instituto Universitario de Investigación en Ciencias Ambientales de Aragón (IUCA), Universidad de Zaragoza, C/ Pedro Cerbuna 12, E-50009 Zaragoza, Spain
[b] Department of Earth Sciences, University College London, Gower Street, London WC1E 6BT, UK
[c] Instituto Geológico y Minero de España, C/ Manuel Lasala 44, 9°B, 50006, Zaragoza, Spain

ARTICLE INFO

Article history:
Received 14 October 2011
Accepted in revised form 13 March 2012
Available online 24 April 2012

Keywords:
Biostratigraphy
Magnetostratigraphy
Campanian
Maastrichtian
Zumaia
Spain

ABSTRACT

The well-exposed and continuous uppermost Cretaceous in the coastal section of Zumaia (northern Spain) crops out as cyclic, deep-water, hemipelagic carbonate-rich sediments of significant geological interest. We present a new, high-resolution calibration of planktonic foraminiferal and calcareous nannofossil biostratigraphic datums, alongside new magnetostratigraphy. Six planktonic foraminiferal zones (*Rugoglobigerina rotundata* to *Pseudoguembelina hariaensis*) and nine nannofossil (sub)zones (UC15e^{TP}? to UC20d^{TP}) have been identified, encompassing the uppermost Campanian through uppermost Maastrichtian. Magnetostratigraphic data were obtained from the lower half of the section, where chrons C31r and C31n have been identified; the lithological nature of the upper part of the section provided spurious palaeomagnetic results. According to these data, the Campanian/Maastrichtian (C/M) boundary lies in Chron C31r at Zumaia. Differences between the planktonic foraminiferal and nannofossil datums at Zumaia and those from the Tercis boundary stratotype section (France) suggest that the biostratigraphic criteria used to identify the C/M boundary are problematic. We propose, therefore, two alternative, key biostratigraphic datums with which to determine the stratigraphic position of this boundary: the stratigraphic base occurrence datum (BO) of the planktonic foraminifer *Pseudoguembelina palpebra* and the top occurrence datum (TO) of the nannofossil *Broinsonia parca* subsp. *constricta*. The C31r/C31n magnetic polarity reversal, and the BOs of the planktonic foraminifer *Racemiguembelina fructicosa* and the nannofossil *Lithraphidites quadratus* are events that may prove useful in formally defining the lower/upper Maastrichtian boundary.

1. Introduction

The Maastrichtian Stage records significant palaeobiological, climatic and oceanographic changes, as well as a meteorite impact event (e.g., Huber and Watkins, 1992; MacLeod et al., 1997; Lees, 2002; Frank et al., 2005; Schulte et al., 2010). The Maastrichtian is informally divided into two substages (lower and upper), but, whilst the Campanian/Maastrichtian (C/M) boundary and the Cretaceous/Paleogene (K/Pg) boundary have been officially defined (Cowie et al., 1989; Odin and Lamaurelle, 2001; Molina et al., 2006), the lower/upper Maastrichtian boundary has not. Detailed and integrated biostratigraphic and chronostratigraphic studies of complete Maastrichtian outcrops are therefore essential in order to supply up-to-date data on potential substage-boundary sections, and to provide supplementary reference data to support the boundary stratotypes.

Studies integrating planktonic foraminiferal and calcareous nannofossil biostratigraphic datums have become standard for aiding in defining and correlating the Upper Cretaceous stage boundaries (e.g., Gale et al., 1996, 2007, 2008), helping to improve stratigraphic resolution on regional scales, at least. However, a useful, fully integrated "global" foraminiferal/nannofossil biozonation scheme for the Upper Cretaceous, that is applicable from shelf to ocean, is elusive, owing to poorly understood palaeobiogeographical constraints acting differentially on each group,

* Corresponding author.
E-mail addresses: irenepr@unizar.es (I. Pérez-Rodríguez), j.lees@ucl.ac.uk (J.A. Lees), jc.larra@igme.es (J.C. Larrasoaña), josearz@unizar.es (J.A. Arz), ias@unizar.es (I. Arenillas).

0195-6671/$ – see front matter © 2012 Elsevier Ltd. All rights reserved.
doi:10.1016/j.cretres.2012.03.011

but also because of a lack of good-quality, integrated datasets. An attempt was made by Bralower et al. (1995), but this is of very low stratigraphic resolution.

The importance to the uppermost Cretaceous of the Zumaia section has been previously recognised, since it is an auxiliary section for the K/Pg boundary (Molina et al., 2009). In addition, Zumaia exhibits alternating limestones and marls, representing orbitally controlled deposition of great interest to cyclostratigraphy (e.g., ten Kate and Sprenger, 1993). These features have potential for use in Maastrichtian astronomical tuning (e.g., Husson et al., 2011), and also for more rigorous calibration of the low-latitude fossil datums with the geological time-scale (GTS of Gradstein et al., 2004; Ogg et al., 2008). Previous multidisciplinary research has been performed on the Maastrichtian of Zumaia, documenting the stratigraphy (e.g., Mount and Ward, 1986; Wiedmann, 1988), ammonites and inoceramids (Ward et al., 1991; MacLeod and Orr, 1993; Ward and Kennedy, 1993), foraminifera (Herm, 1965; Lamolda, 1983; Arz and Molina, 2002), nannofossils (Burnett et al., 1992a; Lamolda and Gorostidi, 1994), carbon and oxygen stable isotopes (Mount et al., 1986; Paul and Lamolda, 2007) and orbital cyclicity (ten Kate and Sprenger, 1993).

Here, we present new biotic data (planktonic foraminifera, nannofossils) from the uppermost Campanian through uppermost Maastrichtian, as well as the first magnetostratigraphy for the lower part of the Maastrichtian for the key section of Zumaia (northern Spain). The aim of this paper is to calibrate the biostratigraphic datums of both micropalaeontological groups with the magnetostratigraphy to provide a robust dataset that contributes to our understanding of the temporal relationships between planktonic foraminiferal and nannofossil stratigraphic events at low latitudes, and that allows the calculation of absolute ages for these datums, for comparison with ages calculated using alternative chronostratigraphic methods, and in different part of the world.

2. Geographical and geological setting

The Zumaia section (43°17′56″N, 2°16′04″W) is located at the Punta Aitzgorri cliff, near the village of Zumaia, Basque Country, northern Spain (Fig. 1). Geologically, the sediments in the section belong to the Upper Cretaceous Zumaia-Algorri Formation (Mathey, 1982), deposited in the Biscay Synclinorium of the Basque-Cantabrian Basin. During the latest Cretaceous, the Basque-Cantabrian Basin was a narrow bay, open to the west, towards the Atlantic, and lying at a palaeolatitude of 30–35°N (Fig. 2), and with a depth of 800–1500 m (Schwentke and Kuhnt, 1992). The basin in general, and the Zumaia section in particular, are characterised by flysch deposits; in the uppermost Cretaceous of Zumaia, these sediments comprise orbitally controlled, alternating hemipelagic limestones and marls (e.g., ten Kate and Sprenger, 1993). The interval studied here corresponds to Lithological Units 2–12 of Wiedmann (1988), and consists of 190.40 m of marls and limestones with intercalated, thin, distal turbidite sandstones (Fig. 3).

The Maastrichtian at Zumaia is very well exposed, seemingly stratigraphically continuous, and represents a high sedimentation rate (Ward, 1988). The section exhibits some faults, but the stratigraphic sequences are easily recognisable in the field.

3. Methods

Slight differences exist between the magnetostratigraphic and micropalaeontological sampling (Fig. 3). For the micropalaeontological analyses, we collected rock samples through ~190 m of the section from 0.43 m (immediately above an evident fault situated in the mid to lower part of Unit 2 of Wiedmann, 1988) to 190.40 m (3 cm below the K/Pg boundary), at around 3 m intervals, but achieving a resolution of 0.25 m around the potential lower/upper Maastrichtian boundary. The samples were taken preferentially from the softer, marly beds, because the foraminifera are easier to extract from this lithology, as opposed to the limestone, without corroding their tests.

3.1. Magnetostratigraphy

The magnetostratigraphic sampling started at the same point as the micropalaeontological sampling, but it was not carried out through the entire section (see reasons below), and all the lithologies were sampled indiscriminately. The magnetostratigraphic study is based on 101 palaeomagnetic samples distributed through the lowermost 89 m of the section studied (Fig. 3). The succession sampled includes whitish limestones and grey marls belonging to Units 2–6 of Wiedmann (1988), as well as the lower half of Unit 7, which is made up of marls ranging in colour from pink to purple. We avoided sampling the upper part of the Maastrichtian succession because previous studies in the neighbouring Sopelana section (Mary et al., 1991; Moreau et al., 1994) have demonstrated that similar purple marls provide spurious palaeomagnetic results, because of complex post-depositional processes. This circumstance does not undermine the interest of our magnetostratigraphic study, since, according to previous biostratigraphic data (Arz and Molina, 2002), the lower part of the section includes the two most relevant events for which magnetochronological data are not yet available: the C/M and lower/upper Maastrichtian boundaries.

One oriented core was taken at each sample location, alternating between limestone and marly levels in Units 2–6, using a portable, gas-powered drill. In the lower half of Unit 7, only purple marls were sampled. This sampling scheme gives a mean resolution of 0.9 m, which allows accurate identification of geomagnetic polarity

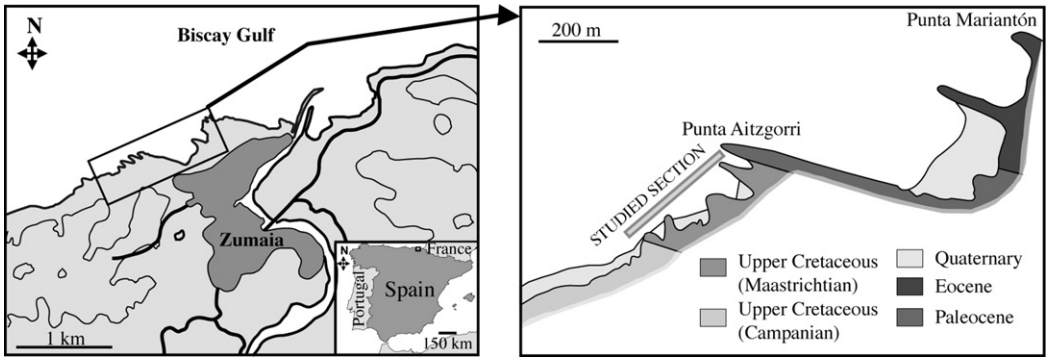

Fig. 1. Location of the village of Zumaia, northern Spain (left), and geological setting of the Zumaia outcrop (right).

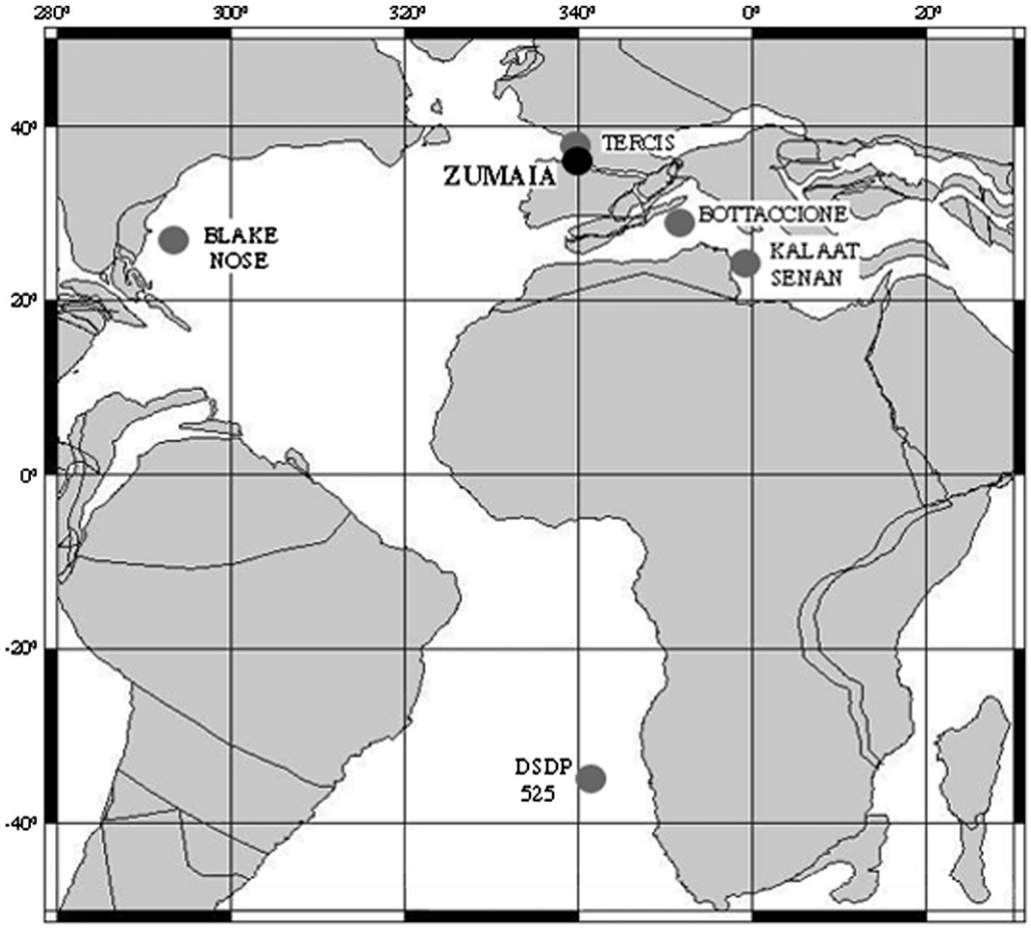

Fig. 2. Palaeogeographical map reconstructed for 68 Ma (modified from http://www.odsn.de/) showing the location of Zumaia (black point) and other low-latitude sections (grey points) discussed in this study.

reversals. Palaeomagnetic analyses were made using a 2G superconducting rock magnetometer at the Palaeomagnetic Laboratory of the Institute of Earth Sciences "Jaume Almera" (CSIC, Universitat de Barcelona), which has a noise level of $<10^{-7}$ A/m for a 10 cm^3 volume of rock. Thermal demagnetization of one specimen per stratigraphic level was done using a MMTD-80 furnace. Thermal treatment involved between 7 and 14 steps, at intervals of 150°, 100°, 50°, 30° and 20 °C, to a maximum temperature of 650 °C. Demagnetization of a set of pilot samples, representative of all the lithologies, allowed optimisation of the demagnetization steps, to allow accurate calculation of the characteristic remanent magnetization (ChRM) directions, minimising heating and formation of new magnetic phases in the oven. ChRM directions were calculated by fitting linear trends in orthogonal demagnetization plots, using the principal component analysis method (Kirschvink, 1980).

3.2. Planktonic foraminifera

Rock samples were crushed with a mortar and then disaggregated by leaving them to stand in dilute (80%) acetic acid for

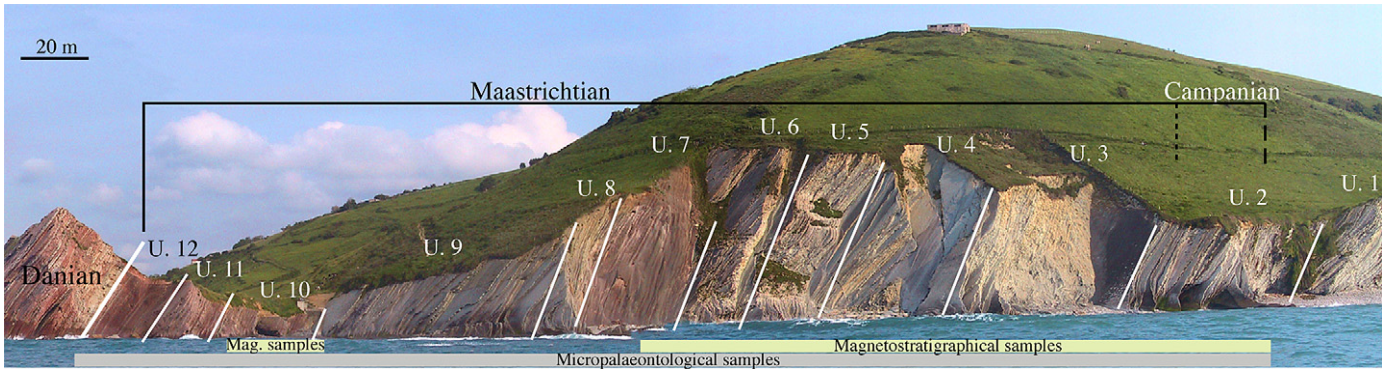

Fig. 3. Panoramic view of the outcrop in the Punta Aitzgorri cliffs, showing the lithological units of Wiedmann (1988), and the extent of the micropalaeontological and magnetostratigraphic sampling.

4 h, following Lirer's (2000) technique to liberate calcareous microfossils from strongly lithified calcareous deposits. The suspension was then washed through a 100-μm-mesh sieve and the >100 μm fraction oven-dried at 50 °C. The >100 μm fraction does not contain as many juvenile taxa as the smaller fractions that are commonly used (i.e., >63 μm); taxonomic identification of these juvenile specimens can be ambiguous. Forty-five samples, from approximately every 5 m (every 1 m through the potential lower/upper Maastrichtian boundary interval), were semi-quantitatively analysed to provide the relative abundance of each species in the assemblages as follows: Abundant, >30%, Common, 30–10%, Few, 10–0.5%, and Rare, <0.5%. Representative specimens of all taxa were picked and mounted onto microslides for a permanent record and for identification purposes. Some specimens were selected for scanning electron microscopy (SEM), using a JEOL JSM 6400 SEM at the Microscopy Service of the Universidad de Zaragoza (Spain). All residues, picked specimens and images are stored in the Departamento de Ciencias de la Tierra (Paleontología), at the Universidad de Zaragoza (Spain).

3.3. Calcareous nannofossils

A total of 49 samples were analysed. Smear-slides were made wherein a surface of the sample was scraped clean with a clean knife, rinsed in tap-water and dried with a clean paper-towel. Sample was scraped from the clean surface, with a clean knife, onto a coverslip that had been licked, so as to stop surface tension preventing smearing of the sediment. A drop of deionised water was added and the powder mixed and smeared, with a flat-sided toothpick, until the sediment was completely broken down (any resistant silt- or sand-sized particles were dragged to one corner of the coverslip and flicked off). The paste was then smeared along the coverslip, so as to provide different thicknesses of sediment, and flash-dried on a hotplate. The coverslip was mounted, sediment-side down, onto a labelled glass slide, using two drops of Norland optical adhesive No. 61, any air-bubbles were pressed out, and the slide was then cured under a UV lamp. This straightforward method of preparation does not skew the components of the nannofloras.

The slides were viewed using a Zeiss Axio Imager.A1 transmitting light microscope, with a polariser, at 1250× magnification. Images were taken using a Leica DFC280 digital camera mounted on the microscope. Five long traverses were made of each slide and the nannofossil relative abundance data recorded semi-quantitatively, using these categories: Common, 1–10 specimens per field of view (fov); Frequent/Few, 1 specimen per <20 fov; Rare, 1 specimen per >20 fov; ?, uncertain identification (owing to poor preservation). Overall abundance (nannofossils versus other particles) was qualitatively estimated using these categories: Very Low, ~<3 specimens per fov; Low, ~3–~10 specimens per fov; and Moderate, ~11 specimens per fov to equal proportion of nannofossils to other sediment. Overall preservation of the nannofloras was also estimated, using these categories: Very Poor, a significant proportion of the assemblage is dissolved and/or a large proportion of specimens are difficult to identify because of secondary calcite overgrowth; Poor, assemblage depleted because of calcite dissolution and/or an appreciable proportion of specimens are difficult to identify because of overgrowth; and Moderate, virtually all specimens are identifiable, although overgrowth has modified the appearance of prone taxa or features (JAL considers this latter to be the "average" state of preservation of Cretaceous taxa). Species richness was tallied for each sample, including all heterococcoliths and nannoliths, but excluding holococcoliths (since these simply represent a different biological phase that probably had a heterococcolith or nannolith counterpart). All sample material, slides and images are stored in the Micropalaeontology Unit at UCL, UK.

4. Results

4.1. Magnetostratigraphy

The palaeomagnetic behaviour of the studied samples is closely linked to the lithology. Grey marls and whitish limestones from Units 2–6 are characterised by a weak natural remanent magnetization (NRM), which is typically lower than 0.2 mA/m (Fig. 4B). For these lithologies, a low-temperature magnetization is unblocked below 240–280 °C, after removal of a viscous component at <150 °C (Fig. 4B). This low-temperature component is parallel to the present-day geomagnetic field at in situ coordinates, and therefore lacks any geological significance for this study. Above 240–300 °C, and up to 460 °C, a ChRM can be identified in about 90% of the samples, despite their overall weak intensities (e.g., samples at 8.09 m, 47.90 m, 63.10 m and 76.17 m in Fig. 4B) (Table 1). According to its unblocking temperatures, this ChRM is interpreted to be carried mainly by magnetite. Marls from Unit 7 have strikingly higher NRM intensities of >2 mA/m, and are also characterised by a viscous component at <150 °C, and/or a low-temperature component, representing a present-day geomagnetic field overprint. Above 400–430 °C, a ChRM with maximum unblocking temperatures exceeding 590 °C, and high intensity, can be identified in most of these marls (e.g., sample at 78.97 m in Fig. 4B, Table 1). According to its maximum unblocking temperatures, this ChRM is interpreted to be carried by hematite.

Three types of ChRM directions have been considered on the basis of their quality (Fig. 4B). Type 1 directions, which represent about 25% of the samples studied, show mostly linear trends directed to the origin of the orthogonal demagnetization plots, although in some cases the growing of new magnetic minerals upon heating prevents full demagnetization (e.g., samples at 47.90 m and 78.97 m in Fig. 4B). These directions have low to moderate errors, which enable accurate calculation of ChRM direction and high-quality polarity determinations. Type 2 directions (40% of the studied samples) show either less well-developed linear trends, or incomplete demagnetizations because of the growth of new minerals during thermal treatment. These directions have errors larger than Type 1 samples, but provide reliable polarity determinations by fitting clustered directions to the origin of the demagnetization plots. Type 3 directions (35% of the studied samples) have highly scattered directions, derived from endpoints observed after removal of the low-temperature component at >240 °C, and provide less reliable polarity determinations.

ChRM directions of samples from Units 2–6 have rather step positive and negative inclinations at in situ coordinates (Fig. 5A, Table 1). After tilt correction, the ChRM has positive and negative inclinations that are similar to the expected Late Cretaceous direction for the studied region (Dec: 001°; Inc: 45; α_{95}: 5.8°; k: 172.3: Larrasoaña et al., 2003) (Figs. 4A and 5A). This indicates that the studied ChRM of Units 2–6 represents a magnetization acquired before folding, which has a Late Eocene age in the studied region (Gómez et al., 2002). Keeping in mind the presence of both northerly and southerly directions, with positive and negative inclinations, respectively, this ChRM is interpreted as a primary remanence acquired at or near deposition. It can therefore be used for establishing a pattern of polarity reversals in the succession studied. ChRM directions of purple marls from Unit 7 have step negative inclinations at in situ coordinates (Fig. 5B, Table 1). After tilt correction, these directions become very similar to the expected Late Cretaceous direction for the region studied (Figs. 4A and 5B), which indicates a prefolding origin. Northerly and positive ChRM

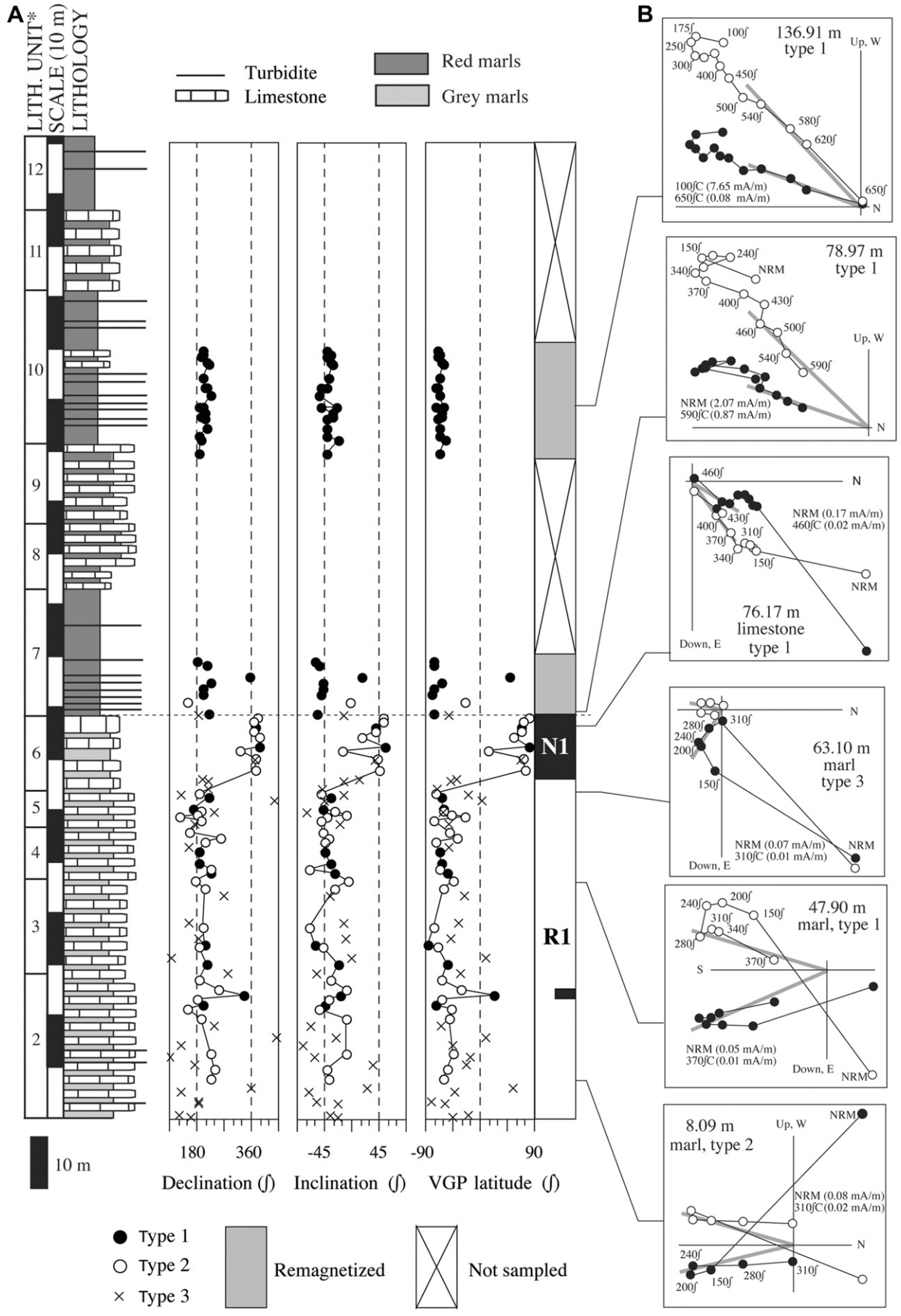

Fig. 4. A, depth variations in declination, inclination and VGP latitude through the Zumaia section. B, orthogonal demagnetization plots (after tilt correction) for representative samples shown as a function of depth. *Lithological units after Wiedmann (1988).

Table 1
Magnetostratigraphic data: BTC, before tilt correction; TC, tilt corrected; MAD, maximum angular deviation; Q, quality type (see text); VGP, virtual geomagnetic pole.

Lith. Unit after Wiedmann (1988)	Height in section (m)	Characteristic remanent magnetization (ChRM)							VGP latitude (°)
		Declination (°) (BTC)	Inclination (°) (BTC)	Declination (°) (TC)	Inclination (°) (TC)	Intensity (10 E-6 A/m)	MAD (°)	Q	
10 pars.	149.72	5.1	−85.1	196.9	−41.8	1055.7	1.2	1	−70.6
	148.82	259.7	−85.6	200.6	−35.0	1797.8	1.4	1	−66.0
	148.32	53.3	−83.0	189.9	−42.4	4427.0	1.3	1	−69.5
	147.42	287.9	−76.9	212.1	−36.4	6772.4	2.3	1	−64.8
	146.82	271.5	−72.6	215.5	−31.0	648.1	5.0	1	−60.4
	144.52	301.8	−86.1	200.5	−38.0	2033.1	4.5	1	−68.0
	142.55	313.7	−79.6	207.9	−41.3	1377.2	3.2	1	−69.3
	142.30	340.8	−70.6	213.6	−51.7	582.2	2.1	1	−74.7
	140.80	334.8	−63.7	225.1	−53.8	630.6	5.0	1	−68.6
	138.80	218.6	−76.6	201.4	−24.5	1085.4	20.3	1	−59.5
	138.57	37.2	−75.8	187.7	−49.9	3872.8	3.3	1	−74.1
	137.48	245.8	−81.6	203.3	−31.4	4633.9	3.1	1	−63.5
	136.91	149.5	−85.1	191.5	−33.5	5084.7	2.2	1	−64.0
	136.45	330.7	−82.6	202.8	−42.1	3309.9	3.4	1	−70.8
	134.57	311.0	−74.8	214.3	−42.1	3412.2	3.2	1	−67.7
	133.10	74.4	−81.2	185.7	−41.2	2259.9	8.4	1	−67.1
	132.10	174.3	−74.6	189.7	−22.5	3388.8	6.0	1	−57.2
9 pars.	129.50	74.9	−83.3	188.2	−40.2	5602.3	0.6	1	−67.4
7 pars.	89.00	31.6	−64.8	181.9	−60.7	1928.4	3.8	1	−76.6
	88.30	348.1	−69.4	212.0	−54.3	408.7	2.7	1	−77.5
	86.20	326.7	61.4	353.6	16.1	65.2	7.6	1	48.0
	85.10	321.0	−66.4	224.6	−47.4	1041.8	3.1	1	−65.4
	84.00	358.4	−76.7	201.8	−49.5	466.7	5.7	1	−77.0
	82.80	0.3	−74.7	202.2	−51.6	2600.5	2.5	1	−78.8
	81.30	128.5	−33.5	145.3	−4.3	68.0	14.2	2	−26.4
	78.97	347.2	−66.2	216.2	−56.5	2001.8	2.6	1	−76.2
6	78.20	186.3	74.4	379.8	52.3	30.4	7.9	2	79.6
	77.42	225.4	74.3	363.6	50.1	28.0	19.0	2	72.0
	76.17	242.8	85.5	371.4	40.0	48.7	10.1	1	68.3
	75.62	267.8	82.5	366.5	39.0	31.9	7.5	2	65.9
	74.40	38.4	66.7	384.8	15.2	12.4	12.6	2	54.2
	72.62	179.3	70.2	385.4	55.6	54.3	4.0	1	81.8
	71.81	319.9	13.7	318.5	−17.1	26.5	8.1	2	13.8
	70.40	232.1	83.8	370.7	41.9	35.5	10.7	2	69.4
	68.10	205.0	80.5	373.5	46.4	48.1	8.5	2	73.5
	63.45	38.8	−73.4	185.3	−51.9	42.1	8.8	2	−74.2
5	62.62	290.3	−73.0	216.9	−36.5	69.8	5.8	1	−63.0
	60.58	66.6	−67.0	168.4	−48.6	59.2	11.4	1	−61.4
	60.08	173.2	−81.2	191.8	−28.8	33.8	12.0	2	−61.2
	59.39	167.9	−58.7	181.5	−8.4	17.0	13.0	2	−47.6
	58.98	77.7	−36.7	125.2	−41.4	45.1	7.7	2	−26.8
	58.30	24.9	−76.5	192.4	−50.3	44.2	6.7	2	−76.3
4	55.80	72.2	−58.9	155.7	−48.0	14.9	10.0	2	−52.0
	54.95	307.5	−41.7	258.0	−38.5	30.8	9.6	2	−37.7
	54.16	347.1	−78.9	203.4	−46.5	26.7	8.8	2	−74.2
	52.34	61.0	−79.3	185.1	−44.1	39.6	8.4	1	−68.7
	49.91	116.2	−82.1	186.2	−35.2	64.7	9.2	1	−63.4
	48.80	0.0	−52.1	227.0	−71.3	37.5	10.5	2	−68.6
	47.90	274.7	−66.2	222.7	−29.3	35.9	5.2	1	−56.2
3	46.34	157.3	−54.9	174.5	−7.6	40.7	8.8	2	−44.5
	45.03	250.9	−79.1	206.0	−30.3	58.4	7.0	2	−62.5
	37.38	15.0	−56.7	196.9	−70.3	25.9	8.6	2	−78.7
	34.21	3.9	−65.3	205.8	−60.8	29.6	2.8	1	−85.5
	33.60	49.3	−75.4	183.6	−48.6	21.0	9.0	2	−71.0
	30.33	249.9	−67.7	215.1	−22.3	46.9	6.5	1	−55.7
2 pars.	27.14	109.7	−80.7	184.3	−35.8	27.0	10.6	2	−63.1
	25.30	268.8	−35.8	247.5	−9.5	9.6	9.5	2	−33.1
	24.30	332.9	20.8	333.3	−19.5	95.2	17.2	1	21.8
	23.50	87.5	−77.1	179.6	−40.0	31.8	18.4	2	−63.4
	22.21	1.2	−80.6	199.1	−46.0	68.1	5.3	1	−74.1
	21.46	60.2	−52.4	146.6	−55.5	22.9	16.4	2	−48.9
	19.56	194.4	−62.8	195.1	−9.8	14.6	12.1	2	−51.4
	12.92	251.5	−50.3	228.2	−10.2	12.1	8.1	2	−44.4
	9.95	309.2	−58.1	237.1	−42.8	34.8	4.3	2	−54.6
	8.09	298.2	−67.0	224.8	−38.4	32.9	5.0	2	−60.1

directions in marls and limestones from Unit 6 shift strikingly to southerly negative directions in purple marls from Unit 7 (Fig. 4A). This shift is accompanied by a marked increase in ChRM intensity, which suggests an underlying remagnetization process (Table 1). Noticeably, the characteristics of such remagnetization (prefolding origin, reverse polarity, higher NRM intensity, ChRM carried by hematite) are identical to those shown by remagnetized purple Maastrichtian marls from the nearby Sopelana section (Mary et al.,

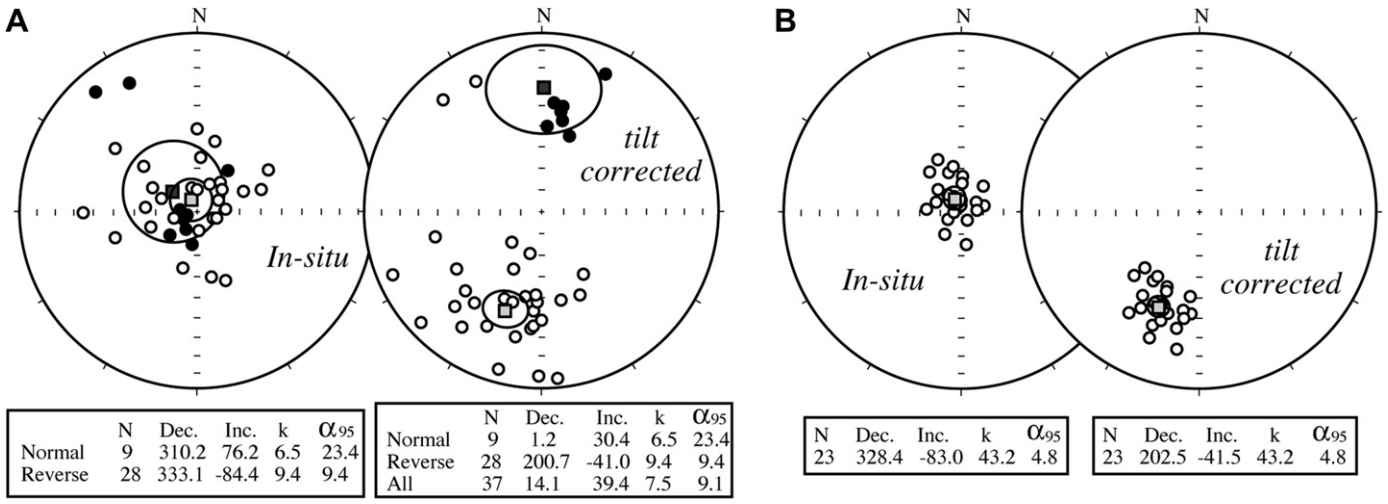

	N	Dec.	Inc.	k	α_{95}
Normal	9	310.2	76.2	6.5	23.4
Reverse	28	333.1	-84.4	9.4	9.4

	N	Dec.	Inc.	k	α_{95}
Normal	9	1.2	30.4	6.5	23.4
Reverse	28	200.7	-41.0	9.4	9.4
All	37	14.1	39.4	7.5	9.1

N	Dec.	Inc.	k	α_{95}
23	328.4	-83.0	43.2	4.8

N	Dec.	Inc.	k	α_{95}
23	202.5	-41.5	43.2	4.8

Fig. 5. A, equal area stereonet projection of ChRM directions from marls and limestones of Units 2–6, which are considered to represent a primary direction. Directions are plotted before and after tilt correction, and are accompanied by ChRM mean directions and their corresponding statistical parameters. B, equal area stereonet projection of ChRM directions from remagnetized marls from Units 7, 9, and 10. Directions are plotted before and after tilt correction, and accompanied by mean directions and their corresponding statistical parameters.

1991; Moreau et al., 1994). The only exception is one sample showing a normal polarity at around 86 m (Fig. 4A). According to the results of Moreau et al. (1994), and in view of its low ChRM intensity (Table 1), this sample is likely to retain a primary magnetization. In order to double-check the occurrence of a remagnetization, we collected 34 additional samples from purple marls from the uppermost part of Units 9 and 10. Biostratigraphic data presented herein places these rocks within the *Abathomphalus mayaroensis* planktonic foraminifera Zone and nannofossil zone UC20a^{TP}; with reference to the Bottaccione (Italy) standard section (Monechi and Thierstein, 1985; Premoli Silva and Sliter, 1995); this constrains the age to Chrons C31n to C30n. The palaeomagnetic behaviour of these marls is identical to that shown by marls from Unit 7, so that they are characterised by even higher NRM and ChRM intensities, and by a reversed-polarity, prefolding ChRM (e.g., sample at 136.91 m in Fig. 4B). These results therefore confirm that the purple Maastrichtian marls from the Zumaia section were remagnetized before the Late Eocene, probably during the Middle Paleocene–Early Eocene (Moreau et al., 1994). Noticeably, the mean ChRM direction of all purple marls, after tilt correction, is rotated 21° clockwise, with respect to the expected Late Cretaceous direction for the region studied (Fig. 5B). This rotation is similar, keeping in mind associated errors, to the 13° of clockwise rotation derived from the primary magnetization isolated in Units 2–6 (Fig. 5A) and to the 17° of clockwise rotation derived from the overlying Paleocene rocks (Dinarès-Turell et al., 2003). Only palaeomagnetic results from Units 2–6 are considered below.

Virtual geomagnetic pole (VGP) latitudes have been calculated, for the sake of quality, using only the most reliable (Type 1 and 2 samples) ChRM directions, after untilting the beds back to their original horizontal position and subtracting the 21° clockwise rotation derived from the remagnetized purple marls, which provide the best-quality data. VGP latitudes indicate the presence of a long reverse magnetozone, labelled R1 (Fig. 5A), which spans from the base of the section (Unit 2) to 65.8 m (lowermost part of Unit 6) (Fig. 4A, Table 1). This magnetozone includes one short, single-sample normal polarity interval, at around 23 m, that has not been considered as a proper magnetozone. The remaining part of Unit 6, and up to the boundary with Unit 7, includes a 12-m-thick normal magnetozone, labelled N1 (Fig. 5A). This interval might be extended at least up into the middle part of Unit 7, keeping in mind the inferred occurrence of a sample retaining a normal polarity direction.

4.2. Planktonic foraminiferal biostratigraphy

The semiquantitative planktonic foraminiferal data for Zumaia are shown in Table 2, alongside the significant datums, interpreted biozones and (sub)stage boundaries. The planktonic foraminiferal biozonation and biostratigraphy are summarised in Fig. 6 and significant planktonic foraminifera taxa are illustrated in Figs. 7 and 8.

Planktonic foraminifera are very abundant in the samples of the studied interval of Zumaia. The highly diverse assemblages that characterise the Maastrichtian basins (Hart, 1999) are recorded at this location, with 16 genera and 71 species identified. These assemblages are dominated by the genera *Heterohelix* and *Globotruncana*.

The specimens from the lower part of the section (from 2.90 m to the top of Unit 6 of Wiedmann, 1988) are less well-preserved than in the upper part. Furthermore, the treatment with acetic acid to retrieve the foraminifera from these well-lithified sediments has partially corroded the ornamentation on the tests (i.e., pustules, costae). This effect is more apparent in some samples than others; for example, in Fig. 8L it is possible to discern meridionally arranged costellae typical of the genus *Rugoglobigerina*, whereas in Fig. 8K, *Rugoglobigerina rotundata* exhibits noticeable corrosion of its typical pustules, even though this specimen possesses all the other typical morphological characteristics of the genus, and the presence of the species is consistent with the Maastrichtian age attributed to the studied section.

The planktonic foraminiferal biozonation proposed and applied herein uses datums/zones from all the planktonic foraminifera families present, as opposed to previous biozonations based on the Family Globotruncanidae (Robaszynski et al., 1984; Caron, 1985), or the Family Heterohelicidae (Nederbragt, 1990). Employing all the families allows a higher-resolution biozonation (e.g., Li and Keller, 1998; Arz and Molina, 2002), and increased ability to correlate between deep and shallower basins, owing to the different life strategies of the different families. The presence of the low-latitude index-species *Gansserina gansseri* and *Plummerita hantkeninoides* has been reported from the Tethyan areas of south-eastern Spain

Table 2
Planktonic foraminifera: stratigraphical distribution, semiquantitative abundance and biostratigraphy, Zumaia. Species having biostratigraphical significance are highlighted in grey. A, abundant; C, common; F, few; R, rare.

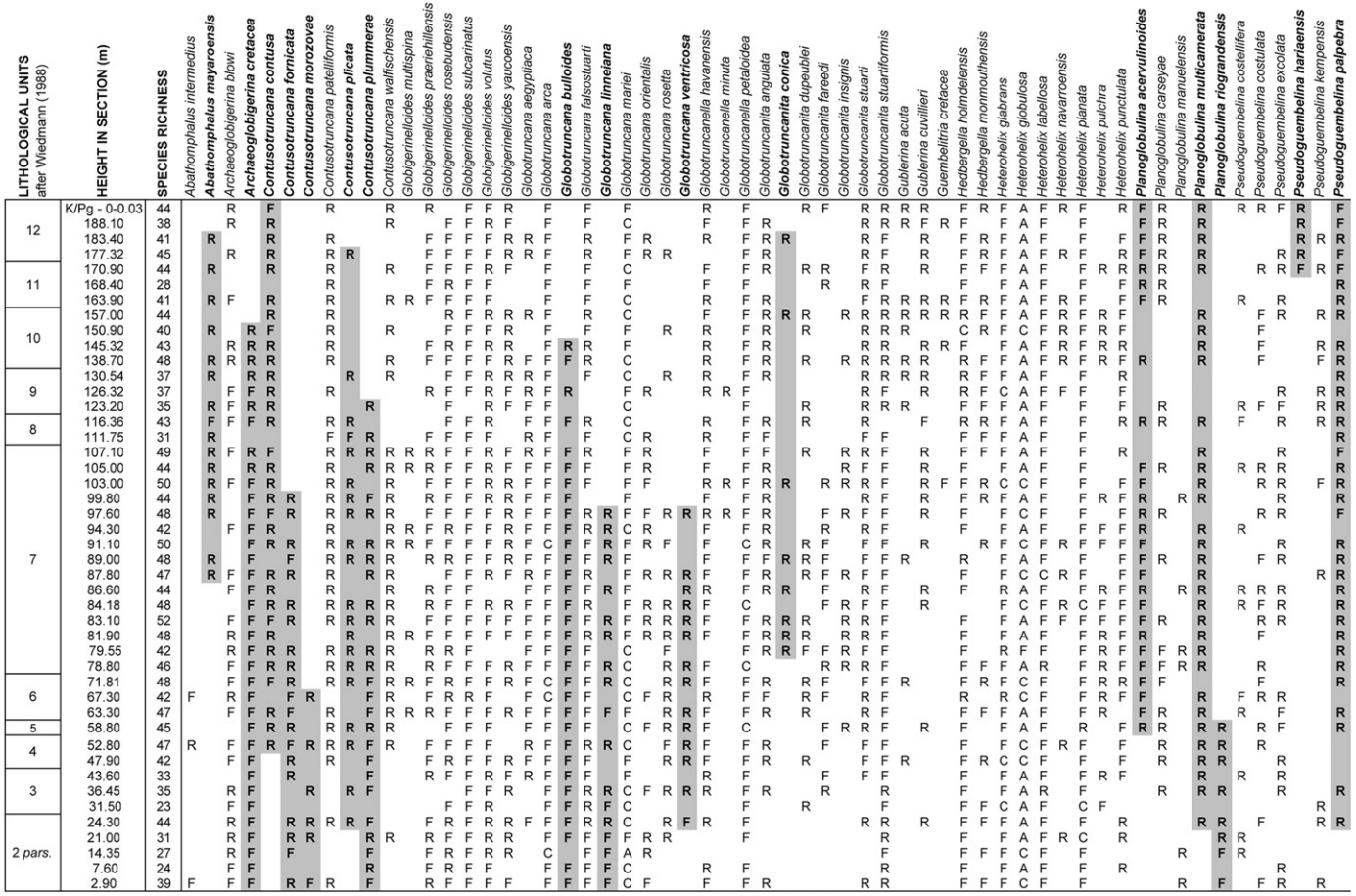

(*continued on next page*)

Table 2 (*continued*)

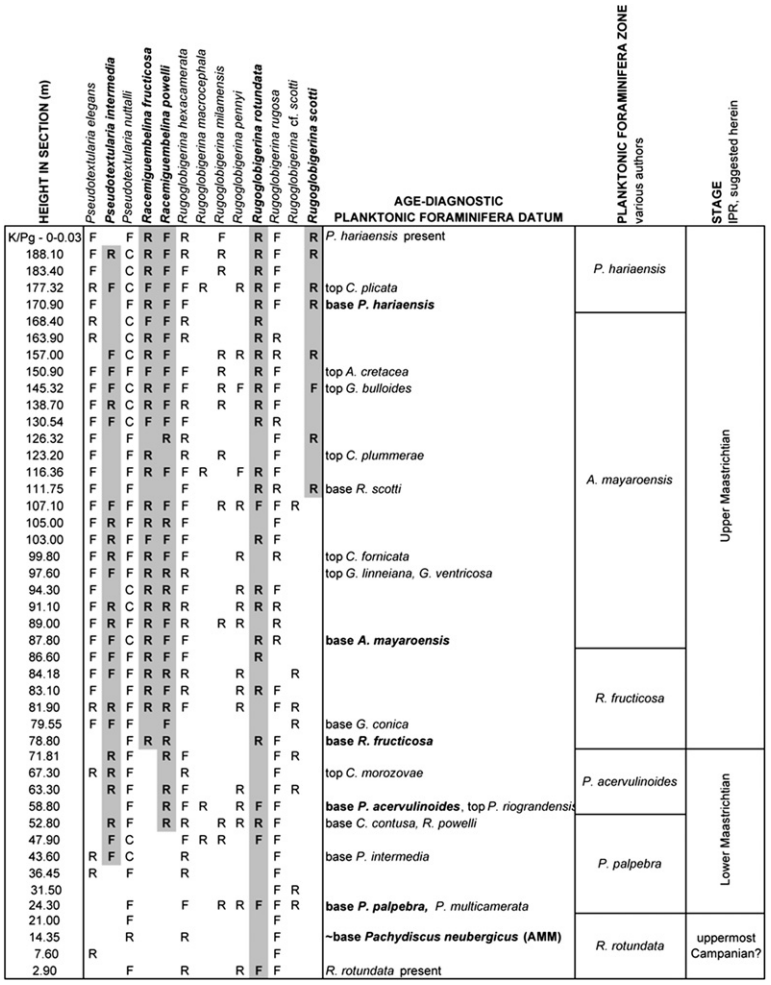

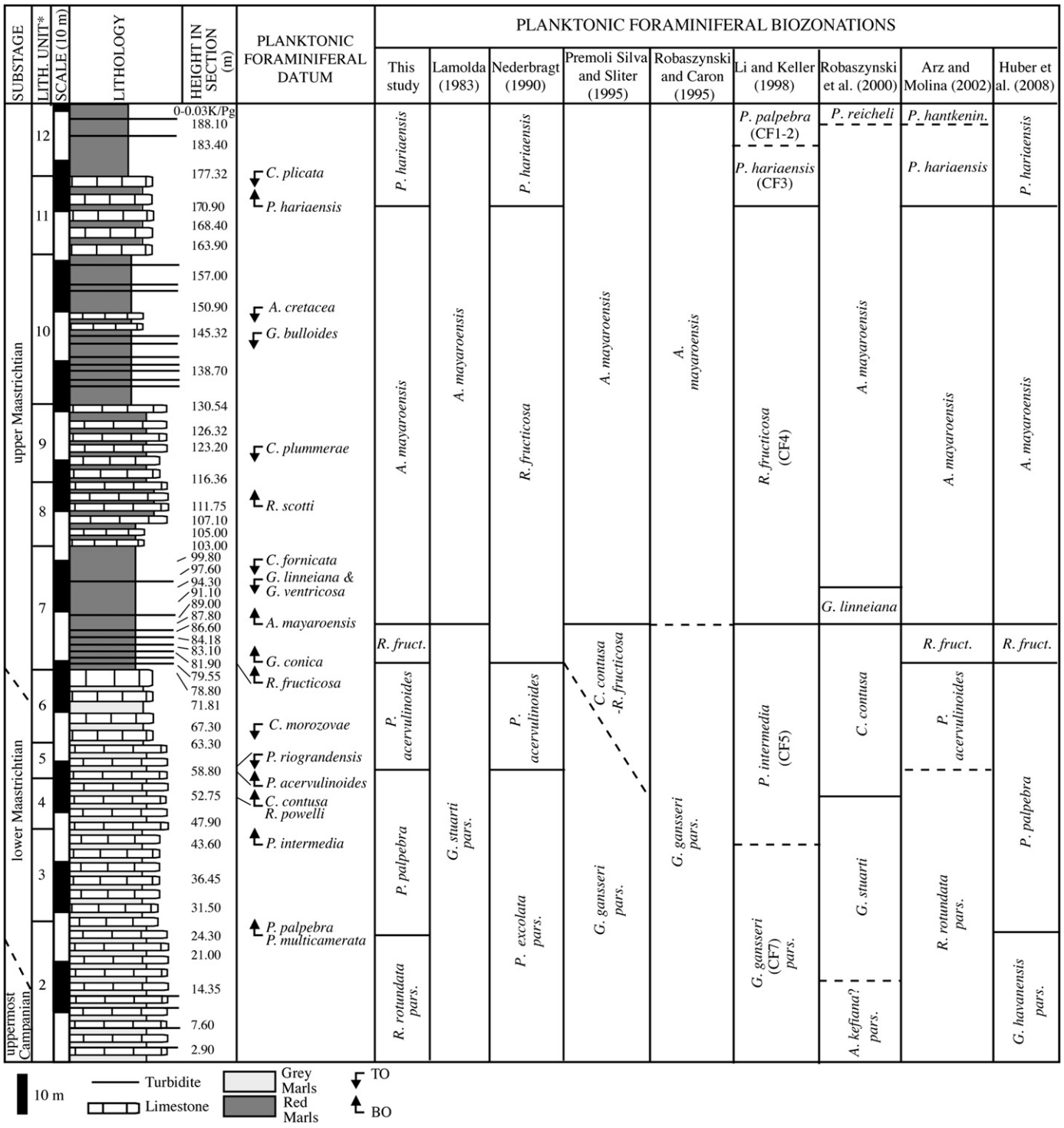

Fig. 6. Summary of the planktonic foraminiferal stratigraphical datums and the proposed biozonation and biostratigraphy for the uppermost Campanian and Maastrichtian of the Zumaia section, compared to other relevant biozonation schemes. Dashed lines indicate that certain datums/biozones are not applicable to Zumaia because of either: (1) the absence of biostratigraphical markers (e.g., *Gansserina gansseri*, as used by Premoli Silva and Sliter (1995), Robaszynski and Caron (1995), and Li and Keller (1998); *Plummerita hantkeninoides*, as used by Arz and Molina (2002); *Plummerita reicheli* and *Archaeoglobigerina kefiana*, as used by Robaszynski et al. (2000)); or (2) a different sequence of stratigraphic datums that leads to a missing zone, such as the *Contusotruncana contusa* Zone (CF6) of Li and Keller (1998) and the *Rugoglobigerina scotti* Zone of Arz and Molina (2002). *Lithological units after Wiedmann (1988).

(Arz et al., 2000; Chacón et al., 2004; Coccioni and Luciani, 2006), but not from the North Atlantic or the Pyrenean Basin (Lamolda, 1983; Arz and Molina, 2002; this study), probably because of palaeobiogeographical differences in distribution. Furthermore, both species are absent (*P. hantkeninoides*) or rare (*G. gansseri*) from Blake Nose (north-western Atlantic) as well (Huber et al., 2008). *Plummerita hantkeninoides* allegedly preferred to live in eutrophic environments above the shelf to upper-slope continental margin and has not been reported from open-ocean pelagic carbonate sediments (Huber et al., 2008, and references cited therein). As

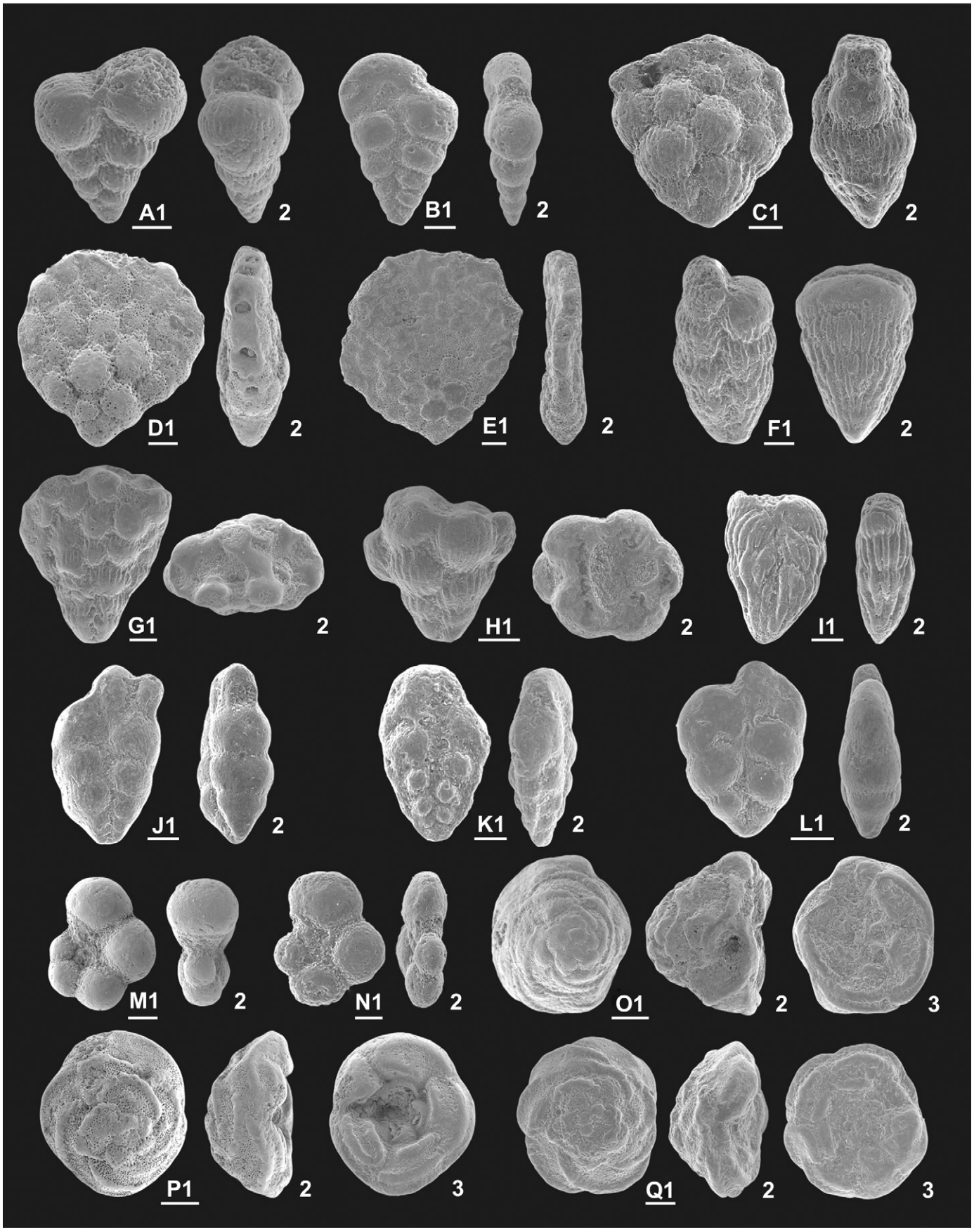

Fig. 7. A1–2, *Heterohelix globulosa*, 99.80 m. B1–2, *Heterohelix planata*, 138.70 m. C1–2, *Planoglobulina acervulinoides*, 188.10 m. D1–2, *Planoglobulina riograndensis*, 55.90 m. E1–2, *Planoglobulina multicamerata*, 52.75 m. F1–2, *Pseudotextularia elegans*, 105.00 m. G1–2, *Racemiguembelina fructicosa*, 105.00 m. H1–2, *Racemiguembelina powelli*, 83.10 m. I1–2, *Pseudoguembelina excolata*, 107.10 m. J1–2, *Pseudoguembelina hariaensis*, 183.40 m. K1–2, *Pseudoguembelina kempensis*, 138.70 m. L1–2, *Pseudoguembelina palpebra*, 83.10 m. M1–2, *Globigerinelloides prairiehillensis*, 91.10 m. N1–2, *Globigerinelloides subcarinatus*, 107.10 m. O1–3 *Contusotruncana contusa*, 87.80 m. P1–3 *Contusotruncana fornicata*, 55.90 m. Q1–3 *Contusotruncana morozovae*, 24.30 m. Scale bar represents 100 μm.

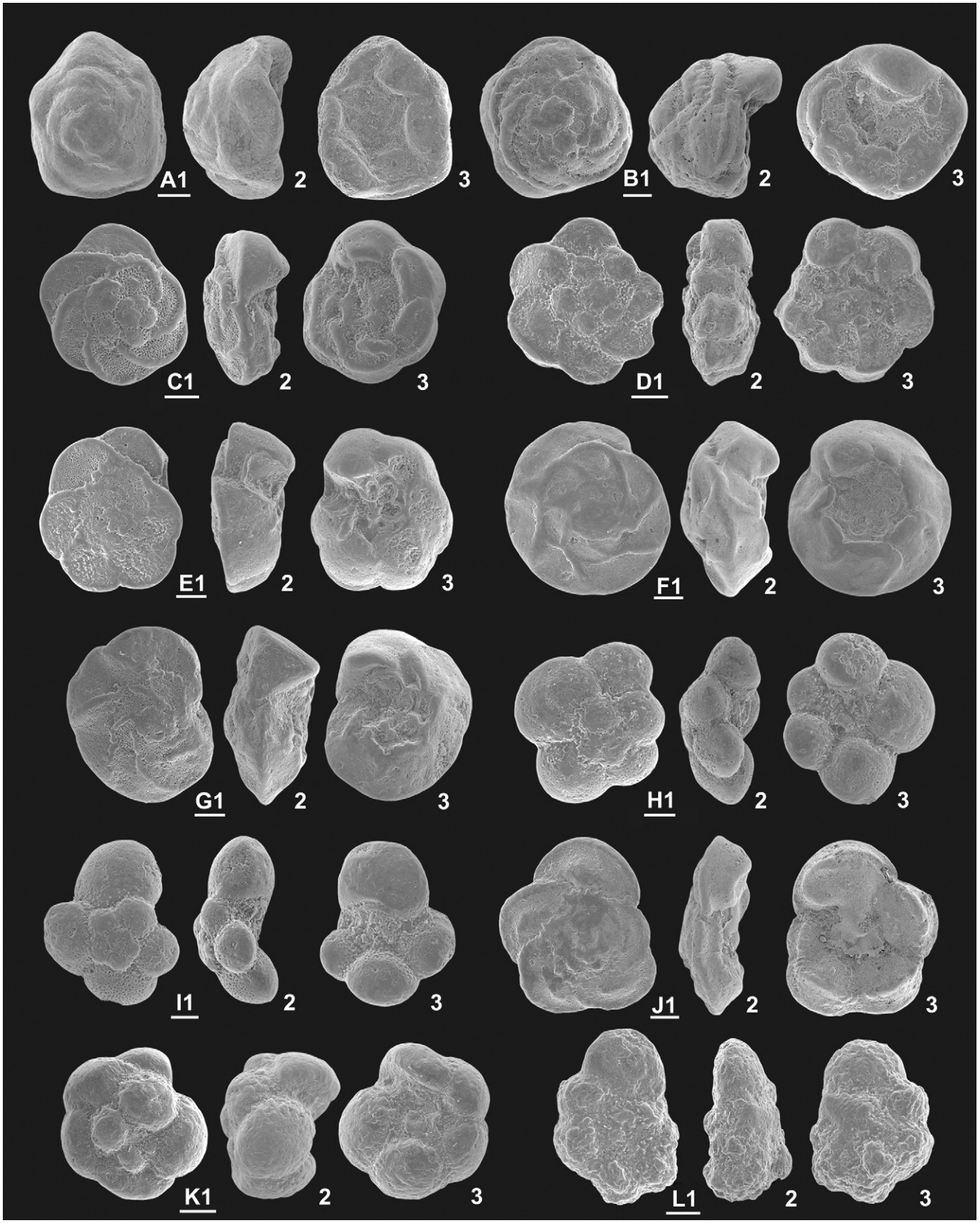

Fig. 8. A1–3, *Contusotruncana patelliformis*, 89.00 m. B1–3, *Contusotruncana walfischensis*, 97.60 m. C1–3, *Globotruncana* cf. *arca*, 97.60 m. D1–3, *Globotruncana bulloides*, 92.13 m. E1–3, *Globotruncanita insignis*, 107.10 m. F1–3, *Globotruncanita stuarti*, 97.60 m. G1–3, *Globotruncanita stuartiformis*, 107.10 m. H1–3, *Globotruncanella havanensis*, 97.6 m. I1–3, *Globotruncanella petaloidea*, 87.80 m. J1–3, *Abathomphalus mayaroensis*, 87.80 m. K1–3, *Rugoglobigerina rotundata*, 83.10 m. L1–3, *Rugoglobigerina scotti*, 145.32 m. Scale bar represents 100 μm.

a consequence of this, low-latitude biozonations (e.g., Li and Keller, 1998; Fig. 6) are difficult to apply to Zumaia and so alternative biozones are proposed here.

Rugoglobigerina rotundata Partial-range Zone
Definition: Interval from the base occurrence (BO) of the nominate species to the BO of *Pseudoguembelina palpebra*.
Author: Modified from Arz and Molina (2001).
Remarks: Several authors record the BO of *R. rotundata* slightly above the BO of *G. gansserina* (e.g., Robaszynski et al., 1984; Arz and Molina, 2002), so this datum is considered useful for locations where *G. gansseri* is biogeographically excluded (see above), such as Zumaia. The top of this zone (i.e., the base of the overlying zone) was originally placed at the BO of *Rugoglobigerina scotti* (Arz and Molina, 2001), whereas here we place it at the BO of *P. palpebra*, because *R. scotti* sensu stricto does not appear at Zumaia until 111.75 m, whilst a form, *R.* cf. *scotti*, occurs at around the level of the BO of *P. palpebra* (Table 2).

The base of this zone is not recorded in this study, since *R. rotundata* is found from the lowermost sample examined (2.90 m). Arz and Molina (2002) placed the base of this zone at Zumaia 154 m below the stratigraphic interval studied here. In this zone, *Heterohelix globulosa* is abundant, and *Heterohelix planata* and *Globotruncana* are common, especially *G. mariei* and *G. arca*. There are no significant micropalaeontological datums recorded in the *R. rotundata* Zone.

Pseudoguembelina palpebra Partial-range Zone
Definition: Interval between the BO of the nominate species and the BO of *Planoglobulina acervulinoides.*
Author: Modified from Huber et al. (2008).
Remarks: See Section 5.2 for further discussion about the biostratigraphical value of *P. palpebra.* Huber et al. (2008) defined their *P. palpebra* Zone based on the BO of *P. palpebra* to the BO of *Racemiguembelina fructicosa*, whereas herein the top of this zone is defined as the BO of *P. acervulinoides* to obtain a higher-resolution biozonation. Previously, Li and Keller (1998) defined a *P. palpebra* Zone with an entirely different connotation, based on the top occurrences (TOs) of *Gansserina gansseri* and *P. palpebra*, but this zone is not applicable herein because of the absence of *G. gansseri.*

The base of this zone lies at 24.30 m at Zumaia. *H. globulosa* is the most abundant species in this zone. *H. glabrans*, *H. planata, Pseudotextularia nuttalli* and *G. mariei* are all common. The BOs of *Planoglobulina multicamerata*, *Pseudotextularia intermedia*, *Contusotruncana contusa* and *Racemiguembelina powelli* are recorded in this zone.

Planoglobulina acervulinoides Partial-range Zone
Definition: Interval from the BO of the nominate species to the BO of *Racemiguembelina fructicosa*.
Author: Nederbragt (1990).
Remarks: At Zumaia, the BO of *P. acervulinoides* is at 58.80 m, in the upper part of Chron C31r, below the BO of the nannofossil *Lithraphidites quadratus.* A similar relative stratigraphic position was recorded at Blake Nose by Huber et al. (2008), in Kalaat Senan (Tunisia) by Robaszynski et al. (2000), and also by Nederbragt (1991) who reported the BO of *P. acervulinoides* in the upper part of the *G. gansseri* Zone. Nevertheless, Premoli Silva and Sliter (1995) placed this datum lower, coincident with the BO of *G. gansseri*, in Chron C32n2n (and, following these authors, Robaszynski and Caron, 1995, gave the same position to the BO of this taxon). We believe that this lower stratigraphic position of the BO of *P. acervulinoides* in the Bottaccione section may be due to a lack of distinction between this species and *P. riograndensis.* The latter is an older species, usually present in low-latitude sections, which is morphologically similar to *P. acervulinoides* but which has fine, vermicular ornamentation and lacks costae. *P. riograndensis* was not recorded at Bottaccione, although there is no biogeographical explanation for its absence there, so we believe these two taxa have been lumped together, because the ornamentation was difficult to recognise in the thin-sections examined by Premoli Silva and Sliter (1995) from Bottaccione. Furthermore, Huber et al. (2008, p. 165) explained the apparent diachroneity between Blake Nose and Bottaccione as possibly the result of "differing taxonomic concepts of this species".

H. globulosa is abundant in this zone, especially in the lower part. Common species are *G. arca*, *G. mariei* and *Globotruncanella petaloidea.* The TOs of *Planoglobulina riograndensis* and *Contusotruncana morozovae* occur in the *P. acervulinoides* Zone.

Racemiguembelina fructicosa Partial-range Zone
Definition: Interval from the BO of the nominate species to the BO of *Abathomphalus mayaroensis*.
Author: Smith and Pessagno (1973).
Remarks: See Section 5.2 for further discussion on the biostratigraphical value of *R. fructicosa.* The base of *R. fructicosa* is at 78.80 m. *H. globulosa* is abundant and *G. mariei*, *G. petaloidea* and *H. planata* are common in this zone. The base of *Globotruncanita conica* is recorded in this zone.

Abathomphalus mayaroensis Partial-range Zone
Definition: Interval from the BO of the nominate species to the BO of *Pseudoguembelina hariaensis*.
Author: Brönnimann (1952), modified by Arz and Molina (2002).
Remarks: See Section 5.2 for further discussion on the biostratigraphical value of *A. mayaroensis.* Brönnimann (1952) originally placed the top of the zone at the K/Pg boundary; subsequently Arz and Molina (2002) changed its top to the BO of *P. hariaensis* to obtain a higher-resolution biozonation.

The BO of *A. mayaroensis* is at 87.80 m at Zumaia. *H. globulosa* is abundant, and *H. glabrans*, *H. labellosa*, *P. nuttalli*, *Hedbergella holmdelensis*, *G. arca*, *G. mariei* and *G. petaloidea* are common in this zone. The TOs of *Globotruncana linneiana*, *G. ventricosa*, *Contusotruncana fornicata*, *C. plummerae*, *G. bulloides* and *Archaeoglobigerina cretacea* are recorded in the *A. mayaroensis* Zone.

Pseudoguembelina hariaensis Partial-range Zone
Definition: Interval from the BO of the nominate species to the K/Pg boundary.
Author: Nederbragt (1990).
Remarks: Robaszynski and Caron (1995) correlated the BO of *P. hariaensis* to Chron C30n, and Li and Keller (1998) reported this datum from the same chron. It is widely accepted that its BO lies above the BO of *A. mayaroensis.*

The BO of *P. hariaensis* is at 170.90 m at Zumaia, and its TO coincides with the K/Pg boundary (virtual top of the studied interval). *H. globulosa* is abundant in this zone, whilst *P. nuttalli* and *G. mariei* are common. The TO of *Contusotruncana plicata* is recorded in this zone.

4.3. Calcareous nannofossil biostratigraphy

All taxa referred to in this study are illustrated and/or referenced in Burnett et al. (1998), supplemented by Lees and Bown (2005), Lees (2007) and Thibault (2010), and all taxa can be found, fully authored, at www.nannotax.org (as of 24.9.2011). Significant taxa are illustrated in Figs. 9–12. Table 3 shows the semiquatitative calcareous nannofossil data; the low-latitude part of the UC biozonation scheme of Burnett et al. (1998, p.158, fig. 6.6) has been applied to this. On Table 3, the biostratigraphically significant taxa

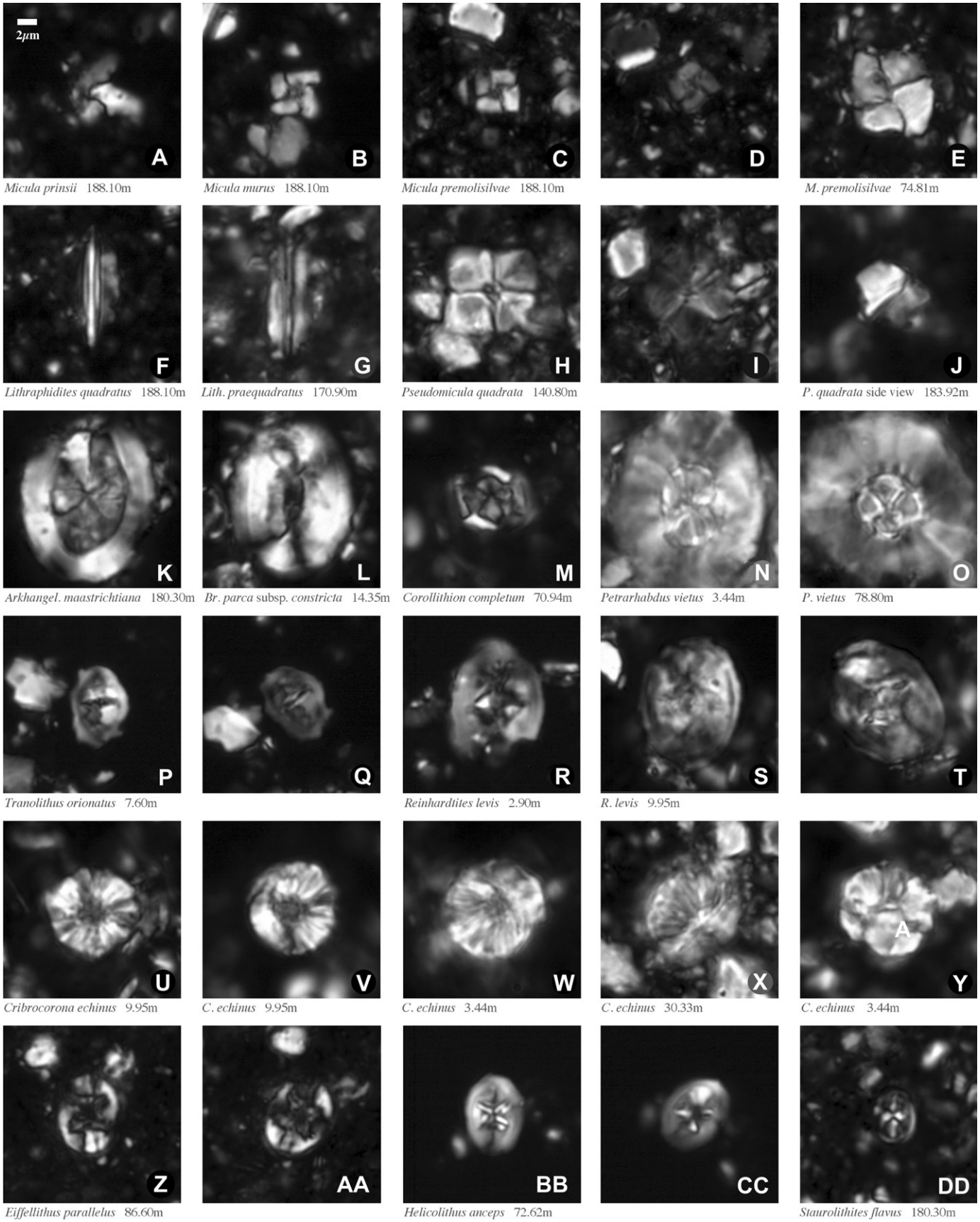

Fig. 9. Nannofossils identified 1.

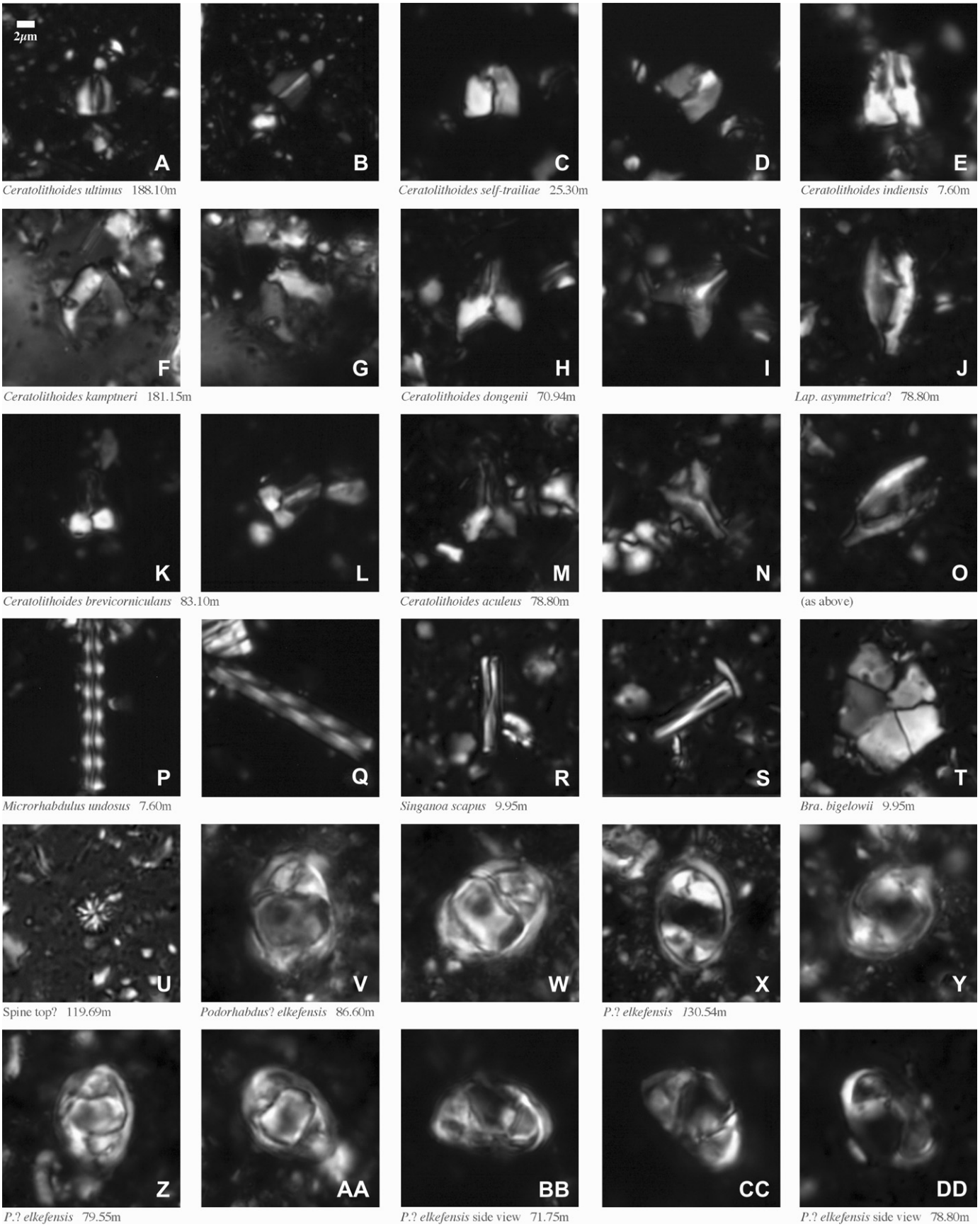

Fig. 10. Nannofossils identified 2.

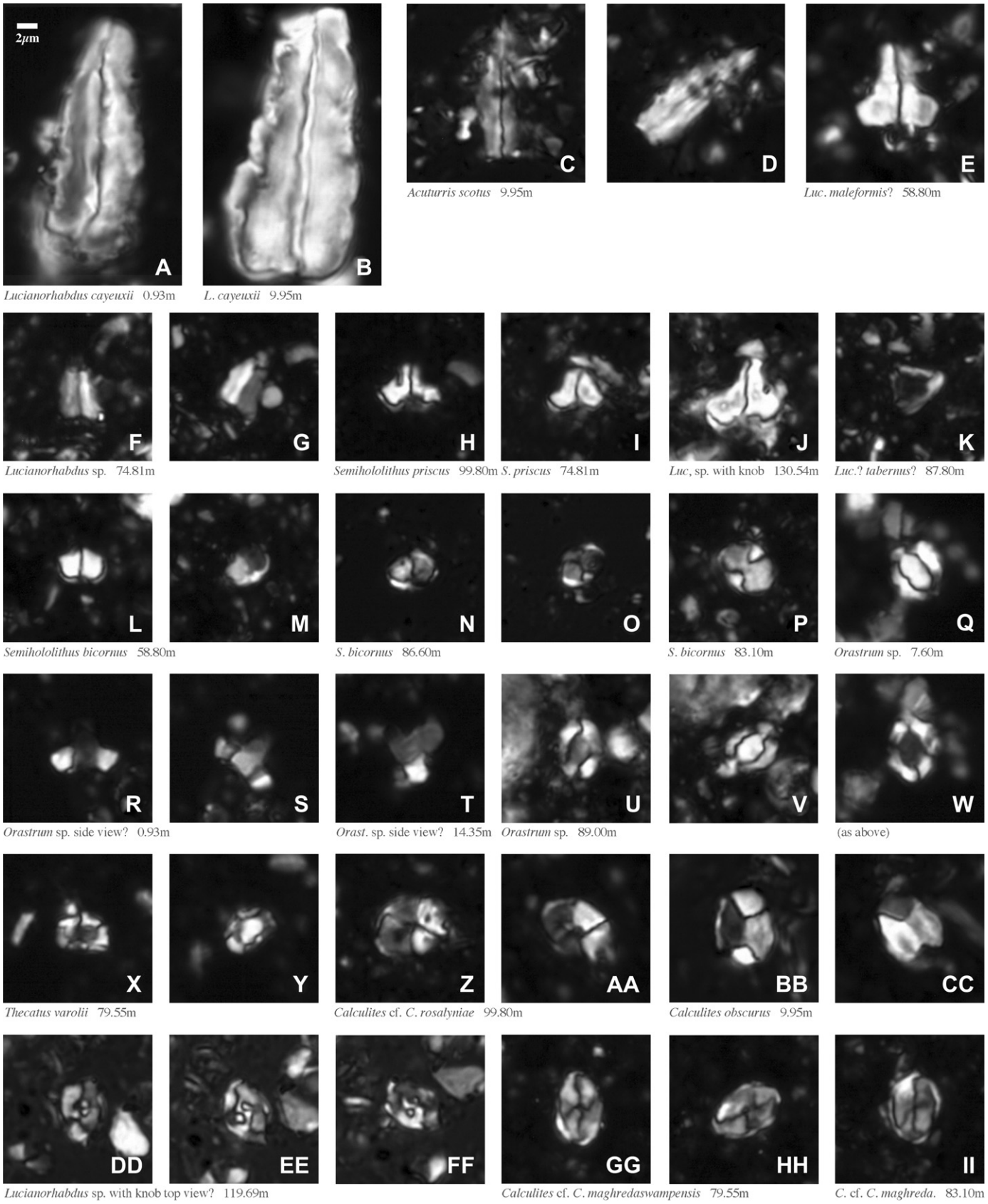

Fig. 11. Nannofossils identified 3.

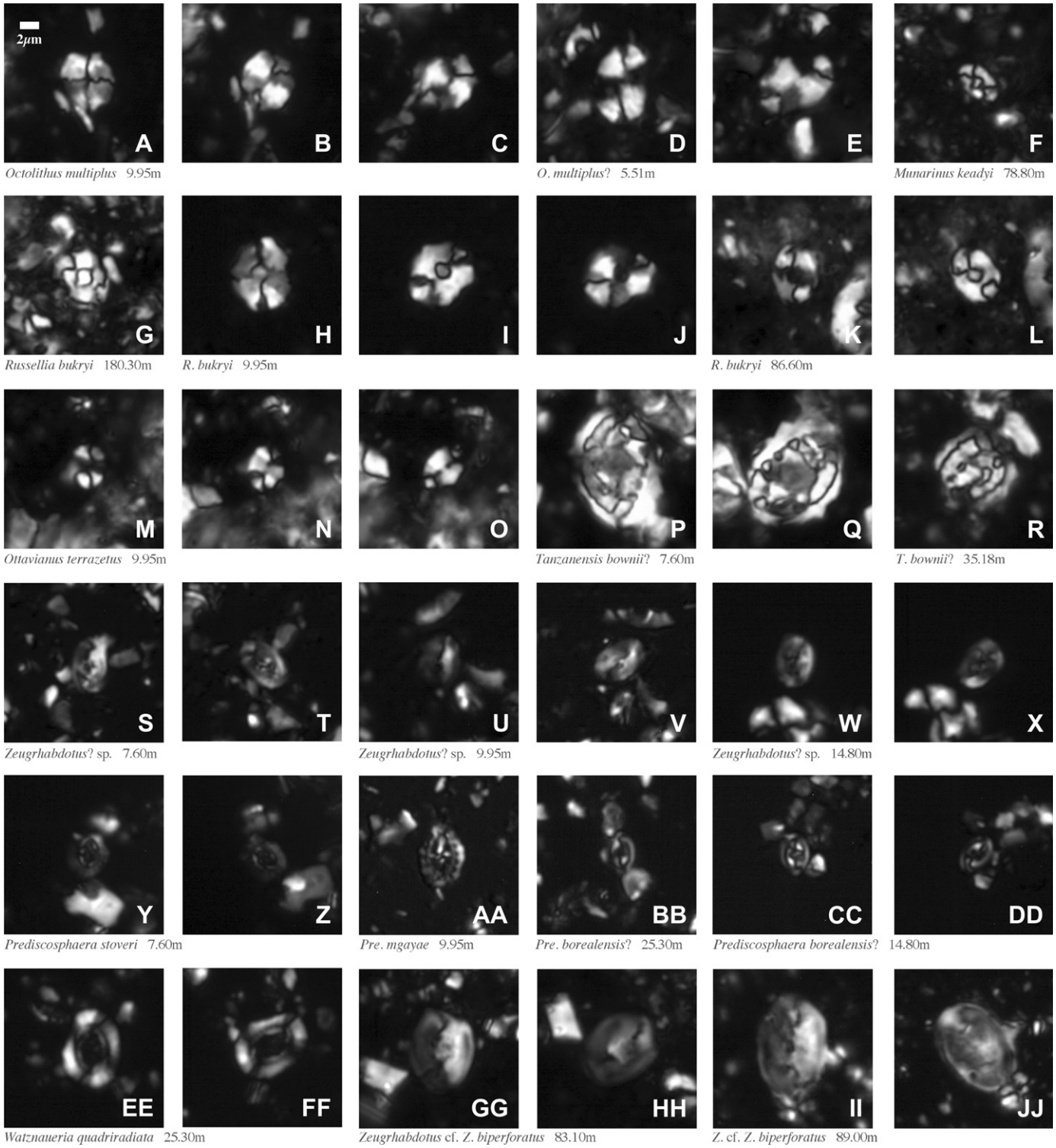

Fig. 12. Nannofossils identified 4.

are highlighted, and a summary of the bioevents used, and the UC zones interpreted from these, is provided on the right-hand side. Preservation of the nannofossils is predominantly very poor to moderate, and overall nannofossil abundances vary from very low to moderate. Despite that, per-sample species richness varies from 31 to 87. Most of these assemblages are probably deleteriously affected by diagenesis (although several holococcolith species, those most prone to post-mortem loss from the assemblage, have survived this), particularly in the lower half of the section (below 80 m), which is dominated by limestones and cemented marls.

The lowest part of the studied Zumaia section is stratigraphically problematic, in nannofossil terms (Figs. 13 and 14). The C/M boundary in the boundary-stratoype section at Tercis (Landes, France) is loosely bracketed by the TOs of *Nannoconus* spp. (below

Table 3

Calcareous nannofossils: stratigraphical distribution, semiquantitative abundance and biostratigraphy, Zumaia. Species having biostratigraphical significance are highlighted in grey. Dark grey highlighting indicates occurrences interpreted as reworked. C, common; F, frequent/few; R, rare; ?, uncertain identification.

(continued on next page)

Table 3 (*continued*)

HEIGHT IN SECTION (m)
K/Pg - 0-0.3
189.76
188.50
188.10
185.90
183.92
181.15
180.30
175.90
170.90
159.80
148.80
140.80
130.54
119.69
110.42
99.80
89.00
87.80
86.60
83.10
79.55
78.80
74.81
72.62
71.75
70.94
63.30
60.08
58.80
49.91
40.21
35.18
30.33
27.14
25.30
22.21
19.56
17.52
15.92
14.80
14.35
9.95
7.60
5.51
3.44
2.90
0.93
0.43
Russellia bukryi side view?
Russellia laswellii
Saepioriyrgata cf. S. bifernia
Semihololithus bicornus
Semihololithus priscus
Semihololithus sp.? top view type 1
Semihololithus sp.? top view type 2
Semihololithus sp.? top view type 3
Serbiscutum gaultensis
Singanoa scapus
Sollasites horticus
Staurolithites sp. with subaxial, bifurcate bars
Staurolithites ellipticus
Staurolithites flavus
Staurolithites haffanii
Staurolithites handleyi
Staurolithites imbricatus
Staurolithites integer
Staurolithites cf. S. laffitei with thick +
Staurolithites laffitei
Staurolithites cf. S. mutterosei
Staurolithites nguru mahambaensis
Tanzanella bowrii top view?
Tetrapodorhabdus decorus
Thecatus cf. T. varolii
Tranolithus gabalus
Tranolithus cf. T. macleodiae
Tranolithus minimus
Tranolithus exiguum
Tranolithus orionatus
Tranolithus cf. T. exiguum with bar
Tranolithus sp.
Tranolithus sp. side view?
Uniplanarius trifidus short form
Watznaueria barnesiae
Watznaueria biporta
Watznaueria diaphanus
Watznaueria cf. W. fossacincta
Watznaueria manivitiae s.l.
Watznaueria cf. W. manivitiae s.l. with central perforation
Watznaueria manivitiae s.s.
Watznaueria ovata
Watznaueria quadriradiata
Zeugrhabdotus acanthus
Zeugrhabdotus bicrescenticus
Zeugrhabdotus bowii
Zeugrhabdotus embergeri
Zeugrhabdotus embergeri very highly-birefringent form
Zeugrhabdotus erectus
Zeugrhabdotus erectus medium-sized form
Zeugrhabdotus moullader
Zeugrhabdotus praesigmoides
Zeugrhabdotus scutula
Zeugrhabdotus trivectis
spine-top?
very small indet. coccoliths
small indet. coccospheres
small indet. calcisphere
distinctive latty calcisphere calcite
AGE-DIAGNOSTIC NANNOFOSSIL DATUM
K taxa present, Danian taxa absent
base M. prinsii
base C. kamptneri
base M. murus
top Petrarhabdus spp.
?base L. quadratus
base A. maastrichtiana
top C. echinus
top R. levis
top Z. bicrescenticus
top A. scutus, ?E. eximius
top T. orionatus
top B. p. constricta
~base Pachydiscus neubergicus (AMM)
top consistent E. eximius, top ?U. trifidus
Reinhardtites anthophorus absent
NANNOFOSSIL ZONE after Burnett et al. (1998)
UC20d TP
UC20c TP
UC20b TP
UC20a TP
UC19
UC18
UC17
UC16
UC15e TP ?
STAGE after Burnett et al. (1998) & suggested herein
upper Upper Maastrichtian
lower to upper Upper Maast.
lower Upper Maastrichtian
upper Lower Maastrichtian
lower Lower Maastrichtian
uppermost Campanian?

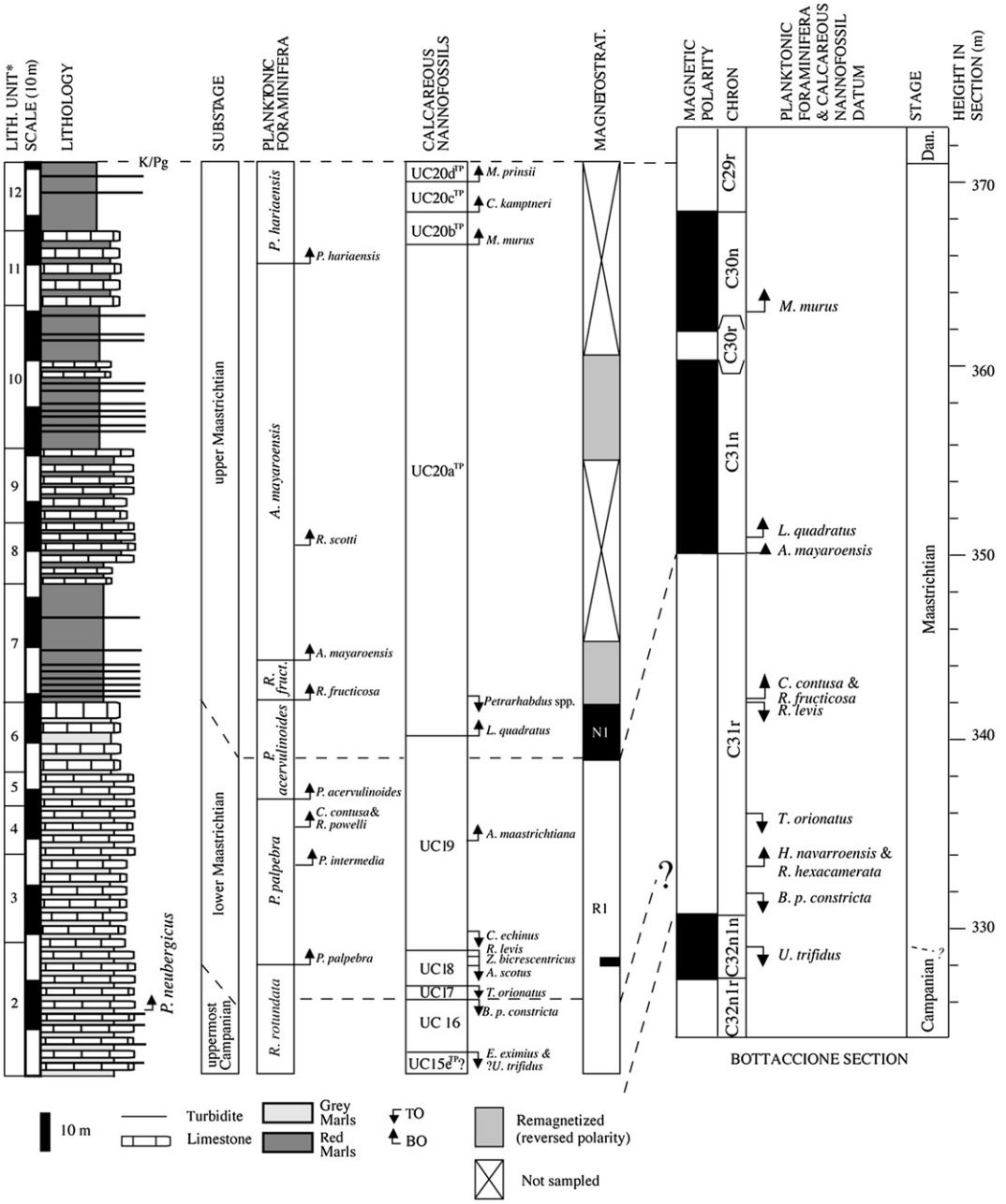

Fig. 13. Summary of the micropalaeontological and magnetostratigraphic datums obtained from Zumaia, showing the (sub)stage boundaries, and correlation with Bottaccione (Premoli Silva and Sliter, 1995). *Lithological units after Wiedmann (1988).

the boundary) at 90.3 m, then above the boundary, *Reinhardtites anthophorus* at ~118 m, *Eiffellithus eximius* at ~124.5 m, *Uniplanarius trifidus* (=*Quadrum trifidum* of some authors) at ~136 m and *Broinsonia parca* subsp. *constricta* at ~166 m (Gardin and Monechi, 2001; Melinte and Odin, 2001; von Salis, 2001). *Nannoconus* spp. and *R. anthophorus* were not recorded at Zumaia. We have recorded two highly questionable specimens of *U. trifidus*, usually a very easily identifiable form, at 3.44 m and 5.51 m. These are very heavily overgrown and may not even be of nannoplankton origin. If these are indeed *U. trifidus*, then the C/M boundary may lie below 5.51 m, with reference to Tercis. However, uncertainty over the placement of the C/M boundary at Zumaia, using nannofossils, is exacerbated by the presence of *E. eximius* from close to the base of the section studied (0.93 m) to 22.21 m, and consistently to 5.51 m. Turbidities are common in the lower ~14 m of the section (see Fig. 4), so it is quite possible that all occurrences of *E. eximius* have been reworked here. This means that the C/M boundary, with respect to the positions of *E. eximius* and *U. trifidus*, cannot be determined at Zumaia (but see Section 5.2, below), and as the datum for the top of Zone UC15e^{TP} (TO *E. eximius*) cannot be trusted here, we have assigned the lowest part of the section to UC15e^{TP}? (between the base of the section and the TO of consistently occurring *E. eximius*), and then UC16 above that level, to the TO of *B. parca* subsp. *constricta*.

There is a "bunching" of nannofossil events between 17.52 m and 30.33 m (top of UC16 through lower UC19). Aside from the zonal marker-species, the TOs of *Acuturris scotus*, *Zeugrhabdotus bicrescenticus* and *Cribrocorona echinus* are worthy of note. It has

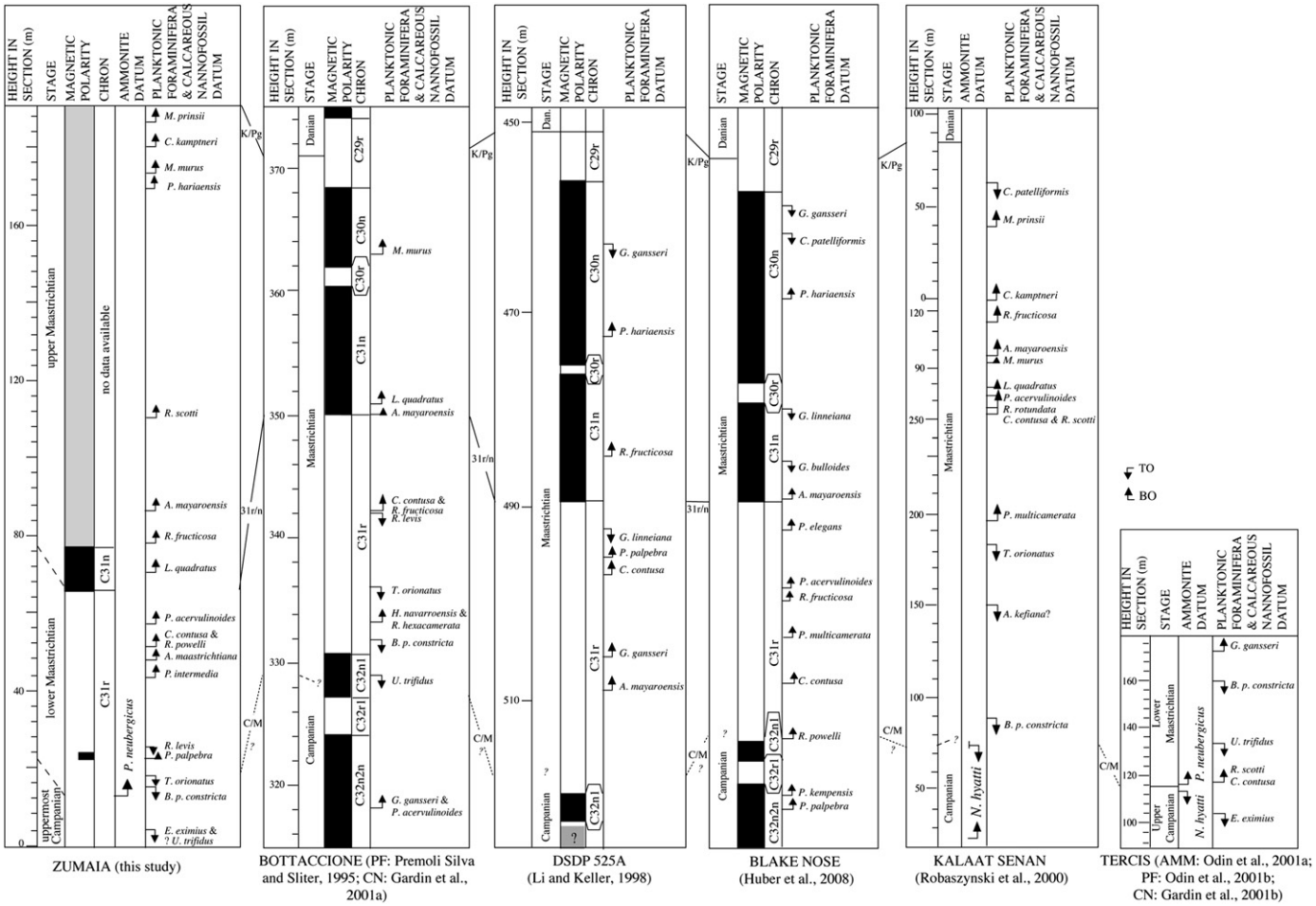

Fig. 14. Comparison of significant stratigraphic datums at Zumaia with those from other low-latitude sections. The position of the events in the Blake Nose scheme was calculated according to an age–depth model (Huber et al., 2008). Note that uncertainties in the datum levels at Tercis are not shown here. A correlation of the Campanian/Maastrichtian boundary in all the sections has been attempted, using datums established at Tercis and observations made in this study.

previously been noted that these taxa disappear around the TO of *Tranolithus orionatus*: in the tropical Indian Ocean, the TO of *A. scotus* approximates the TO of *T. orionatus* (Lees, 2002); in the tropical Pacific Ocean, the TO of *C. echinus* lies at the same level or above the TO of *T. orionatus*, and the TO of *Z. bicrescenticus* lies above both (Lees and Bown, 2005). These taxa may prove to have wide (global low-latitude) stratigraphic and correlative value.

The BO of *Arkhangelskiella maastrichtiana* (at 49.91 m) is used to define the base of subzone UC20c^{BP} in the northern high-latitude part of the zonation of Burnett et al. (1998). At Zumaia, its base is below this level, below the BO of *Lithraphidites quadratus*, which itself defines the base of UC20a^{TP} and UC20a^{BP}, in the low- and northern high-latitude parts of the Burnett et al. (1998) biozonation, respectively.

The BO of *L. quadratus*, previously highlighted as a potential marker for the lower/upper Maastrichtian boundary (Paul and Lamolda, 2007) lies at 71.75 m or 72.62 m, the lower occurrence being a single, very poorly preserved specimen, and so questionable.

The biostratigraphy of the upper part of the section is quite straightforward: all the low-latitude marker-taxa datums/zones are present. This probably reflects the switch to predominantly marly lithologies (see Fig. 4, Table 3). Another datum of note is the TO of *Petrarhabdus* spp. in UC20a^{TP}. This was also noted by Burnett (in Burnett et al. (1998); Lees, 2002) in the Indian Ocean, and it may prove to have wider stratigraphic and correlative utility.

5. Discussion

5.1. Magnetostratigraphy and correlation to the "standard" section at Bottaccione, Italy

Correlation of the lower half of the Zumaia section to Bottaccione is relatively straightforward, based on the simple pattern of polarity reversal relative to key biostratigraphical datums (Fig. 13). Interval R1 contains the BO of the planktonic foraminifer *C. contusa*, which lies in Chron C31r at Bottaccione (Premoli Silva and Sliter, 1995). This calibration is confirmed by the TOs of the nannofossils *B. parca* subsp. *constricta*, *T. orionatus* (=*T. phacelosus* of some authors) and *R. levis* that are also recorded in this chron at Bottaccione (Gardin et al., 2001a). The BO of *L. quadratus* lies close to the C31r/C31n reversal boundary at Zumaia in the normal chron, as it does at Bottaccione (Monechi and Thierstein, 1985; Gardin et al., 2001a). So, it seems reasonable that we ascribe our interval N1 at Zumaia to C31n.

5.2. The Campanian/Maastrichtian boundary at Zumaia

The earliest definition of the Maastrichtian Stage was given by Dumont (1849) for a detrital carbonate deposit with Maastricht (southern Netherlands) as its type locality; the stratotype was fixed near this town, in a quarry at St. Pietersberg. However, these

sediments are affected by a hiatus at the C/M boundary (Jagt, 2001). Nowadays, the C/M boundary is officially defined as lying at 115.2 m on platform IV of the quarry at Tercis les Bains (France), having been ratified in 2001 (Odin and Lamaurelle, 2001). This level is the arithmetic mean of 12 biotic datums of alleged equal importance that serve as biostratigraphic criteria. These include the BO of the ammonite *Pachydiscus neubergicus*, the TOs of the ammonite *Nostoceras hyatti* and the nannofossil *Uniplanarius trifidus* (=*Quadrum trifidum* of some authors), and the BOs of the planktonic foraminifera *Rugoglobigerina scotti* and *Contusotruncana contusa*.

We discuss the sequence of events across the Campanian/Maastrichtian boundary at Zumaia below.

Consistent TO of the calcareous nannofossil *Eiffellithus eximius* and questionable TO of the calcareous nannofossil *Uniplanarius trifidus* at 5.51 m.

In nannofossil terms, at Tercis, the C/M boundary has been shown to lie below the TO of *U. trifidus* and also below the older TOs of *E. eximius* and *Reinhardtites anthophorus* and above the TO of *Nannoconus* spp. (combined data of Gardin and Monechi, 2001; Melinte and Odin, 2001; von Salis, 2001), that is, in zone UC15e^{TP}. *U. trifidus* is questionably present at Zumaia (see Section 4.3, above), and *R. anthophorus* is not stratigraphically present, but *E. eximius* is, and so it is not possible to identify the boundary at Zumaia, using these datums. Note that there is also widespread evidence of the TO of *U. trifidus* lying above the TO of *B. parca* subsp. *constricta*, as highlighted, for example, by the CC biozonation of Sissingh (1977), as modified by Perch-Nielsen (1985), and the UC biozonation of Burnett et al. (1998), and so the validity of its use as in indicator of the C/M boundary outside of Tercis, and perhaps particularly in more open marine sediments, is questionable, since its range at Tercis may be prematurely truncated.

BO of the ammonite *Pachydiscus neubergicus* at ~14 m.

This event was recorded ~30 m above a waterfall, just at the transition from more to less indurated sediments, and some metres below a prominent limestone bed that is easily recognisable in the field (Ward and Kennedy, 1993). Based on a comparison of the gross features of our lithological log (e.g., Fig. 4) with those of Ward and Kennedy's (1993, p. 8, fig. 5), the BO of *P. neubergicus* lies at ~14 m in our section, close to the top of the interval with turbidites. It should be noted that the next specimen of *P. neubergicus* recorded by Ward and Kennedy (1993) occurs at ~44 m in our section (based on visual correlation of our log with theirs); this paucity of ammonite data may suggest that we cannot reliably use this datum to identify the C/M boundary at Zumaia.

TO of the calcareous nannofossil *Broinsonia parca* subsp. *constricta* at 17.52 m.

The C/M boundary at Tercis is closely bracketed by the TO of the ammonite *Nostoceras hyatti* (below the boundary) and the BO of the ammonite *P. neubergicus* (see Odin et al., 2001a, p. 827, fig. 1). Burnett et al. (1992b) showed the TO of *B. parca* subsp. *constricta* to lie between these two events, that is, very close to the boundary. In nannofossil terms, the boundary would thus lie in lowest UC17, below the TO of *Tranolithus orionatus*. Elsewhere, the BO of *P. neubergicus* has been shown to lie between the TO of *Eiffellithus eximius* (older datum) and the TO of *B. parca* subsp. *constricta*, that is, in UC16 (e.g., Hancock et al., 1993; Wagreich et al., 1998, 2003). Thus, it is demonstrably clear that the TO of *B. parca* subsp. *constricta* approximates the C/M boundary. At Zumaia, the BO of *P. neubergicus* (at ~14 m) lies within ~4 m of the TO of *B. parca* subsp. *constricta* (at 17.5 m), thus within Zone UC16, and so the level of this ammonite datum (and also this nannofossil datum) is probably consistent with the level of the C/M boundary here.

BO of the planktonic foraminifer *Pseudoguembelina palpebra* at 24.30 m.

In this study, this event is proposed as an approximator of the C/M boundary at Zumaia. Nederbragt (1991) pointed out that the BO of *P. palpebra* occurred in the middle of the *Gansserina gansseri* Zone that spans this boundary; and even though it apparently exhibits some diachroneity [Li and Keller (1998) placed its BO in the upper part of Chron C31r at DSDP Hole 525A, and Huber et al. (2008) reported its BO lying in C32n2n at Blake Nose; Fig. 14], it seems a reasonable local index for the C/M boundary, at least, being ~10 m above the BO of *P. neubergicus* at Zumaia.

BO of the planktonic foraminifera *Contusotruncana contusa* at 52.75 m.

This event is a primary biotic datum marking the C/M boundary at Tercis but appears not to be applicable at Zumaia because we record it too high in the section, coincident with *R. powelli*, in the *Pseudoguembelina palpebra* Zone, and well above the level of the C/M boundary, relative to other datums. The position of this datum at Zumaia is consistent with that of Lamolda (1983) in the Basque-Cantabrian Basin, and our report of the BO of *C. contusa* in Chron C31r concurs with its placement there by Premoli Silva and Sliter (1995) in the Bottaccione section, Li and Keller (1998) in the mid-latitude South Atlantic DSDP Hole 525A, and Huber et al. (2008) in Blake Nose (Fig. 14). Robaszynski et al. (2000) also recorded its BO well above the C/M boundary (identified based on the TO of the ammonite *Nostoceras hyatti*) in Kalaat Senan, Tunisia (Fig. 14). However, identification of the BO of *C. contusa* could be problematic. Robaszynski and Mzoughi (2010) pointed out that it is difficult to distinguish precisely between *C. contusa* and its predecessor, *C. patelliformis*, since there is a morphological continuum between the species. In addition, some of the characteristics used to differentiate between these related taxa (i.e., test conicity, number of chambers) have been demonstrated to be latitude-dependent (Kucera and Malmgren, 1996). For all these reasons, *C. contusa* does not seem an appropriate biostratigraphic marker for the C/M boundary.

BO of the planktonic foraminifer *Rugoglobigerina scotti* at 111.75 m.

In common with *C. contusa*, this species is a primary biotic datum marking the C/M boundary at Tercis, but it is also not applicable to Zumaia because its BO is reported too high in the section, well above the C/M boundary, relative to other datums. The position of this datum at Zumaia is consistent with that reported by Lamolda (1983) in the Basque-Cantabrian Basin. Robaszynski et al. (2000) also found its BO at a stratigraphically higher level at Kalaat Senan (Tunisia), at the same level as *C. contusa* (Fig. 14). The BO of *R. scotti* at Tercis is somewhat controversial, because the specimen illustrated by Arz and Molina (2001, p. 347, pl. 2, figs. 4, 5), from 116.8 m, is a primitive form, not representative of the typical morphology of the species. For that reason, that specimen was considered to be *R.* cf. *scotti* (Odin et al., 2001a, p. 828), although this is not reflected in the summary figure (Odin et al., 2001a, p. 827, fig. 1). Linares (1977) had previously distinguished between two morphotypes of the species in southern Spanish sections, naming the youngest morphotype *Trinitella scotti* (=*R. scotti*), and the more primitive morphotype *T.* cf. *scotti*. At Zumaia, we found *R.* cf. *scotti* from 24.30 m (Table 2, Fig. 6); as these transitional forms do not strictly adhere to the original description, we do not consider them to be useful for identifying the C/M boundary at Zumaia.

Magnetostratigraphy of the C/M boundary.

If we believe that the record of *P. neubergicus* reported by Ward and Kennedy (1993) accurately represents its BO and that the TO of *Broinsonia parca* subsp. *constricta* lies a short distance above this, then the C/M boundary lies in Chron C31r at Zumaia (Fig. 13).

However, this highlights a potential stratigraphical problem: an attempt to calculate a correlation of the Tercis section with Bottaccione resulted in the BO of *P. neubergicus*, and thus the C/M boundary, being placed in Chron C32n2n (Odin, 2001, p. 779, fig. 2), and this is where Husson et al. (2011) placed the C/M boundary through astronomical tuning, using the TO of *Uniplanarius trifidus* as a calibration point. There is room for error in these calculations, particularly considering the differences in sedimentation rates between Tercis and Bottaccione, and the use of the TO of *Uniplanarius trifidus* as a calibration point, which we have already highlighted above as being potentially diachronous.

There is obviously a need for more stratigraphic data from the C/M boundary interval, particularly from low latitudes, to document clearly relative diachrony between fossil datums associated with this boundary and to shed light on the palaeobiogeographic constraints controlling the order of biostratigraphic datums of the different fossil groups. Furthermore, we introduce uncertainty in the calibration of the C/M boundary with the magnetostratigraphical scale, and so we recommend detailed magneto/biostratigraphcal studies through this interval, particularly in sections where *P. neubergicus* has been recorded, in order to provide a clear-cut calibration.

5.3. Towards a definition for the lower/upper Maastrichtian boundary

At the "Second International Symposium on Cretaceous Stage Boundaries" in Brussels in 1995, division of the Maastrichtian stage into two substages was recommended. However, there is still no formal agreement for the placement of a lower/upper Maastrichtian boundary. The Zumaia section was proposed as a potential substage-boundary stratotype (Odin et al., 1996), but a practical definition of this boundary at Zumaia is still pending. Several biotic datums were suggested as potential markers of this boundary, including the extinction of rudist reefs, the virtual extinction of inoceramids, the BOs of an unspecified calcareous nannofossil and the ammonite *Pachydiscus fresvillensis*.

Fig. 14 shows a comparison of significant stratigraphic datums at Zumaia with those from other low-latitude sections, and below we discuss the sequence of events across the lower/upper Maastrichtian boundary at Zumaia.

C31r/C31n palaeomagnetic reversal at 65.8 m.

This event would be very useful to define the lower/upper Maastrichtian boundary. It has the advantage of being isochronous and valid for different depositional environments.

BO of *Lithraphidites quadratus* at 71.75 m.

This datum is recorded in Wiedmann's (1988) Unit 6, 6 m above the base of Chron C31n (Fig. 13). The BO of *L. quadratus* at Zumaia is lower than has been previously reported: Paul and Lamolda (2007) indicated its BO in low Unit 7; however, this level probably equates to its first few/frequent occurrence at Zumaia (see Table 3), coincident with better preservation in more marly sediments. *L. quadratus* is widely distributed geographically, although it can be vanishingly rare at northern high latitudes (e.g., Sheldon, 2008) and is absent from southern high latitudes (e.g., Watkins et al., 1996; Lees, 2002). It lies in C31n at Zumaia (herein), Bottaccione (Monechi and Thierstein, 1985; Gardin et al., 2001a) and at DSDP Site 527 (JAL, unpubl. data, 2003). Its BO, close to that of *R. fructicosa* and the C31r/C31n magnetic reversal, make it an acceptable candidate for defining the substage boundary, at least at low to mid latitudes.

BO of *Racemiguembelina fructicosa* at 78.80 m.

There are some concerns about the isochrony of the BO of *R. fructicosa*: it has been recorded above the C31r/C31n palaeomagnetic reversal herein (Fig. 13) and Li and Keller (1998) placed this in Chron C31n in the South Atlantic mid-latitudes (DSDP Hole 525A; Fig. 14), whereas at Blake Nose (western North Atlantic: Huber et al., 2008; Fig. 14) and Bottaccione (Premoli Silva and Sliter, 1995) it has been placed lower, in Chron C31r (Fig. 14). This discrepancy could be a result of biogeographic controls in its distribution, or to taxonomic factors, such as lumping the intermediate forms in with *R. fructicosa* sensu stricto. Indeed, Huber et al. (2008, p. 169) stated that "the presence of [older] intermediate forms may cause some uncertainty in identifying this datum", and the discrepancy highlighted here with Premoli Silva and Sliter (1995), who identified taxa from thin-sections in which it is sometimes difficult to identify taxa reliably, may be owing to a lack of distinction between *R. fructicosa* and its ancestor, *R. powelli*, in the older specimens from Bottaccione. Both species have an initial biserial arrangement, followed by a number of multiserial chambered sets; however, *R. powelli* differs from *R. fructicosa* in having one to two multiserial sets, instead of four to five sets (Nederbragt, 1991). Specimens with three multiserial sets are scarce, and must be included in *R. powelli*, according to its type description (Smith and Pessagno, 1973). The only specimen figured as *R. fructicosa* by Premoli Silva and Sliter (1995, pl. 26, fig. 7), recorded in Chron C31r, possesses six chambers in cross-section, so should be reassigned to *R. powelli*; this figured specimen is not listed in the distribution chart and lies below the *R. fructicosa* Zone established by them. Since the taxonomic distinction between *R. powelli* and *R. fructicosa* is clear, even when there is a complete range of morphotypes between these species (Nederbragt, 1989), we conclude that the BO of *R. fructicosa* is a robust datum with which to identify and correlate the lower/upper Maastrichtian boundary at low latitudes, since *R. fructicosa* is easily identifiable and common in tropical and subtropical regions, although it should be noted that it is rare at high (southern) latitudes (Southern Ocean: Huber, 1992; Petrizzo, 2001).

BO of *Abathomphalus mayaroensis* at 87.80 m.

Paul and Lamolda (2007) reported the BO of this species to lie in the upper part of Unit 7; in this study we record it lower, probably because of our higher-resolution sampling (Table 2). Its common occurrence is consistent with the point where Paul and Lamolda (2007) recorded its BO. The BO of *A. mayaroensis* (=base of the *A. mayaroensis* Zone) is often used to divide the Maastrichtian into two substages. This taxon exhibits a discontinuous stratigraphic distribution that seems to be dependent on specific environmental conditions; thus Odin et al. (2001, p. 830) noted that *A. mayaroensis* is a poor index-species for global correlation, because it is rare or absent in tropical regions and shallow-water environments, and its BO is demonstrably diachronous, depending on latitude. The BO of *A. mayaroensis* is recorded well above the C31r/C31n palaeomagnetic reversal at Zumaia, and has been reported from Chron C31n at Blake Nose, North Atlantic (Huber et al., 2008) and Sopelana, Spain (Mary et al., 1991), but it has been found to lie in Chron C31r in mid to southern high latitudes of the South Atlantic (Barrera and Huber, 1990; Huber and Watkins, 1992; Li and Keller, 1998). At Bottaccione, Premoli Silva and Sliter (1995) placed this datum coincident with the base of Chron C31n. This different stratigraphical position at Zumaia could be due to either a diachronous BO from Bottaccione to Zumaia or a taxonomic problem: Premoli Silva and Sliter (1995) found *A.* cf. *mayaroensis* coincident with the base of Chron C31n and *A. mayaroensis* sensu stricto three samples higher; in this case, the BO of *A. mayaroensis* may also lie above the magnetic reversal at Bottaccione.

6. Conclusions

New magnetic polarity, planktonic foraminiferal and calcareous nannofossil data from the Zumaia section have allowed us to establish an integrated sequence of stratigraphic datums for the uppermost Campanian through the Maastrichtian.

The main conclusions of this study are: (1) the BO of the planktonic foraminifer *Pseudoguembelina palpebra* and the TO of the nannofossil *Broinsonia parca* subsp. *constricta* are useful, alternative key datums for the identification of the C/M boundary, since the defining criteria proposed at Tercis seem not to be applicable at Zumaia; (2) the position of the C/M boundary at Zumaia lies within Chron C31r; (3) only the lower part of the Zumaia section produces meaningful palaeomagnetic data, and the C31r/C31n magnetic reversal is located at 65.8 m; (4) since Zumaia is a candidate substage-boundary stratotype for the lower/upper Maastrichtian boundary, we propose as potential defining criteria: (a) the C31r/C31n magnetic reversal at 65.8 m; (b) the BO of the calcareous nannofossil *Lithraphidites quadratus* at 71.75 m; and (c) the BO of the planktonic foraminifer *Racemiguembelina fructicosa* at 78.80 m.

Acknowledgements

This research was funded by the Aragonian Departamento de Educación y Ciencia (DGA grupo EO5), by the Spanish Ministerio de Educación y Ciencia projects CGL2007–63724/BTE and CGL2011–22912, and co-financed by the ERDF (European Regional Development Fund). IPR is supported by a FPI grant (BES–2008–006773), funded by the Spanish Ministerio de Educación y Ciencia. This work was carried out whilst JAL was funded by NERC grant NE/G004986/1. We thank Marcos Lamolda for his help and taxonomic advice. We are grateful to Asier Hilario for providing the panoramic photograph in Fig. 3. The two anonymous reviewers are thanked for their time and for suggesting several useful improvements to the manuscript.

References

Arz, J.A., Molina, E., 2001. Planktic foraminiferal quantitative analysis across the Campanian/Maastrichtian boundary at Tercis les Bains (France). In: Odin, G.S. (Ed.), The Campanian–Maastrichtian Stage Boundary: Characterisation at Tercis les Bains (France) and Correlation with Europe and other Continents. Developments in Palaeontology and Stratigraphy, vol. 19. Elsevier, Amsterdam, pp. 338–348.

Arz, J.A., Molina, E., 2002. Bioestratigrafía y cronoestratigrafía con foraminíferos planctónicos del Campaniense superior y Maastrichtiense de latitudes templadas y subtropicales (España, Francia y Tunicia). Neues Jahrbuch für Geologie und Paläontologie, Monatshefte 224, 161–195.

Arz, J.A., Arenillas, I., Molina, E., Sepúlveda, R., 2000. La estabilidad faunística de los foraminíferos planctónicos en el Maastrichtiense superior y su extinción en masa catastrófica en el límite K/T de Caravaca (España). Revista Geológica de Chile 27, 27–50.

Barrera, E., Huber, B., 1990. Evolution of Antarctic waters during the Maestrichtian: foraminifer oxygen and carbon isotope ratios, Leg 113. Proceedings of the Ocean Drilling Program, Scientific Results 113, 813–827.

Bralower, T.J., Leckie, R.M., Sliter, W., 1995. An integrated Cretaceous microfossil biostratigraphy. In: Berggren, W.A., Kent, D.V., Aubry, M.-P., Hardenbol, J. (Eds.), Geochronology, Time Scales and Global Stratigraphic Correlation. SEPM Special Publication, vol. 54, pp. 65–79.

Brönnimann, P., 1952. Globigerinidae from the Upper Cretaceous (Cenomanian–Maastrichtian) of Trinidad. Bulletin of American Paleontology 34 (140), 1–30.

Burnett, J.A., (with contributions from Gallagher, L.T., and Hampton, M.J.), 1998. Upper Cretaceous. In: Bown, P.R. (Ed.), Calcareous Nannofossil Biostratigraphy. British Micropalaeontologicasl Society Publications Series. Chapman and Hall/Kluwer Academic Publishers, London, pp. 132–199.

Burnett, J.A., Hancock, J.M., Kennedy, W.J., Lord, A.R., 1992b. Macrofossil, planktonic foraminiferal and nannofossil zonation at the Campanian/Maastrichtian boundary. Newsletters on Stratigraphy 27, 157–172.

Burnett, J.A., Kennedy, W.J., Ward, P.D., 1992a. Maastrichtian nannofossil biostratigraphy in the Biscay region (south-western France, northern Spain). Newsletters on Stratigraphy 26, 145–155.

Caron, M., 1985. Cretaceous planktonic foraminifera. In: Bolli, H.M., Saunders, J.B., Perch–Nielsen, K.P. (Eds.), Plankton Stratigraphy. Cambridge University Press, Cambridge, pp. 17–86.

Chacón, B., Martín–Chivelet, J., Gräfe, K.U., 2004. Latest Santonian to latest Maastrichtian planktic foraminifera and biostratigraphy of the hemipelagic successions of the Prebetic Zone (Murcia and Alicante provinces, south-east Spain). Cretaceous Research 25, 585–601.

Coccioni, R., Luciani, V., 2006. *Guembelitria irregularis* bloom at the K–T boundary: morphological abnormalities induced in planktonic foraminifera by impact-related extreme environmental stress? In: Cockell, C., Koeberl, C., Gilmour, I. (Eds.), Biological Processes Associated With Impact Events. Impact studies. Springer-Verlag, Berlin, pp. 179–196.

Cowie, J.W., Ziegler, W., Remane, J., 1989. Stratigraphic Commission accelerates progress, 1984 to 1989. Episodes 12, 79–83.

Dinarès-Turell, J., Baceta, J.I., Pujalte, V., Orue-Etxebarria, X., Bernaola, G., Lorito, S., 2003. Untangling the Palaeocene climatic rhythm: an astronomically calibrated Early Paleocene magnetostratigraphy and biostratigraphy at Zumaia (Basque Basin, northern Spain). Earth and Planetary Science Letters 216, 483–500.

Dumont, A.H., 1849. Rapport sur la carte géologique du Royaume. Bulletin de l'Academie Royale des Sciences des Lettres et des Beaux-Arts 16, 351–373.

Frank, T.D., Thomas, D.J., Leckie, R.M., Arthur, M.A., Bown, P.R., Jones, K., Lees, J.A., 2005. The Maastrichtian record from Shatsky Rise (northwest Pacific): a tropical perspective on global ecological and oceanographic changes. Paleoceanography 20, PA1008. doi:10.1029/2004PA001052.

Gale, A.S., Hancock, J.M., Kennedy, W.J., Petrizzo, M.R., Lees, J.A., Walaszczyk, I., Wray, D.S., 2008. An integrated study (geochemistry, stable oxygen and carbon isotopes, nannofossils, planktonic foraminifera, inoceramid bivalves, ammonites and crinoids) of the Waxahachie Dam Spillway section, north Texas: a possible boundary stratotype for the base of the Campanian Stage. Cretaceous Research 29, 131–167.

Gale, A.S., Kennedy, W.J., Burnett, J.A., Caron, M., Kidd, B.E., 1996. The Late Albian to Early Cenomanian succession at Mont Risou near Rosans (Drôme, SE France): an integrated study (ammonites, inoceramids, planktonic foraminifera, nannofossils, oxygen and carbon isotopes). Cretaceous Research 17, 515–606.

Gale, A.S., Kennedy, W.J., Lees, J.A., Petrizzo, M.R., Walaszczyk, I., 2007. An integrated study (inoceramid bivalves, ammonites, calcareous nannofossils, planktonic foraminifera, stable carbon isotopes) of the Ten Mile Creek section, Lancaster, Dallas County, north Texas, a candidate Global boundary Stratotype Section and Point for the base of the Santonian Stage. Acta Geologica Polonica 57, 113–160.

Gardin, S., Monechi, S., 2001. Calcareous nannofossil distribution in the Tercis geological site (Landes, SW France) around the Campanian–Maastrichtian boundary. In: Odin, G.S. (Ed.), The Campanian–Maastrichtian Stage Boundary: Characterisation at Tercis les Bains (France) and Correlation with Europe and other Continents. Developments in Palaeontology and Stratigraphy, vol. 19. Elsevier, Amsterdam, pp. 272–284.

Gardin, S., del Panta, F., Monechi, S., Pozzi, M., 2001a. A tethyan reference record for the Campanian and Maastrichtian stages: the Bottaccione section (Central Italy); review of data and new calcareous nannofossil results. In: Odin, G.S. (Ed.), The Campanian–Maastrichtian Stage Boundary: Characterisation at Tercis les Bains (France) and Correlation with Europe and other Continents. Developments in Palaeontology and Stratigraphy, vol. 19. Elsevier, Amsterdam, pp. 745–757.

Gardin, S., Odin, G.S., Bonnemaison, M., Melinte, M., Monechi, S., von Salis, K., 2001b. Results of the cooperative study on the calcareous mannofossils across the Campanian–Maastrichtian boundary at Tercis les Bais (Landes, France). In: Odin, G.S. (Ed.), The Campanian–Maastrichtian Stage Boundary: Characterisation at Tercis les Bains (France) and Correlation with Europe and other Continents. Developments in Palaeontology and Stratigraphy, vol. 19. Elsevier, Amsterdam, pp. 293–309.

Gómez, M., Vergés, J., Riaza, C., 2002. Inversion tectonics of the northern margin of the Basque Cantabrian Basin. Bulletin de la Société Géologique de France 173, 449–459.

Gradstein, F., Ogg, J., Smith, A., 2004. A Geologic Time Scale 2004. Cambridge University Press, Cambridge, 589 pp.

Hancock, J.M., Peake, N.B., Burnett, J., D'Hondt, A.V., Kennedy, W.J., Stokes, R.B., 1993. High Cretaceous biostratigraphy at Tercis, southwest France. Bulletin de l'Institut Royal des Sciences Naturelles de Belgique, Sciences de la Terre 63, 133–148.

Hart, M.B., 1999. The evolution and biodiversity of Cretaceous planktonic Foraminiferida. Geobios 32, 247–255.

Herm, D., 1965. Mikropaläontologisch-stratigraphische untersuchungen im Kreideflisch zwischen Deva und Zumaya (prov. Guipúzcoa, Nordspanien). Zeitschrift der Deutschen Geologischen Gesellschaft 115, 277–348.

Huber, B.T., 1992. Paleobiogeography of Campanian–Maastrichtian foraminifera in the southern high latitudes. Palaeogeography, Palaeoclimatology, Palaeoecology 92, 325–360.

Huber, B.T., Watkins, D.K., 1992. Biogeography of Campanian–Maastrichtian calcareous plankton in the region of the Southern Ocean: paleogeographic and paleoclimatic implications. In: Kennet, J.P., Warnke, D.A. (Eds.), The Antarctic paleoenvironment; a perspective on global change. Antarctic Research Series, vol. 56, pp. 31–60.

Huber, B.T., MacLeod, K.G., Tur, N.A., 2008. Chronostratigraphic framework for upper Campanian–Maastrichtian sediments on the Blake Nose (subtropical North Atlantic). Journal of Foraminiferal Research 38, 162–182.

Husson, D., Galbrun, B., Laskar, J., Hinnov, L.A., Thibault, N., Gardin, S., Locklair, R.E., 2011. Astronomical calibration of the Maastrichtian (Late Cretaceous). Earth and Planetary Science Letters 305, 328–340.

Jagt, J.W.M., 2001. The historical stratotype of the Maastrichtian: a review. In: Odin, G.S. (Ed.), The Campanian–Maastrichtian Stage Boundary: Characterisation at Tercis les Bains (France) and Correlation with Europe and other Continents. Developments in Palaeontology and Stratigraphy, vol. 19. Elsevier, Amsterdam, pp. 711–722.

Kirschvink, J.L., 1980. The least-squares line and plane and the analysis of paleomagnetic data. Geophysical Journal of the Royal Astronomical Society 62, 699–718.

Kucera, M., Malmgren, B.A., 1996. Latitudinal variation in the planktic foraminifer *Contusotruncana contusa* in the terminal Cretaceous ocean. Marine Micropaleontology 28, 31–52.

Lamolda, M.A., 1983. Biostratigraphie du Maastrichtien vasco-cantabrique; ses foraminifers planctoniques. Géologie Méditerranéenne 10, 121–126.

Lamolda, M.A., Gorostidi, A., 1994. Nanoflora y acontecimientos del tránsito Cretácico–Terciario. Una visión desde la región Vascocantábrica. Revista de la Sociedad Mexicana de Paleontología 7, 45–58.

Larrasoaña, J.C., Pares, J.M., del Valle, J., Millán, H., 2003. Triassic paleomagnetism from the western Pyrenees revisited; implications for the Iberian–Eurasia Mesozoic plate boundary. Tectonophysics 362, 161–182.

Lees, J.A., 2002. Calcareous nannofossil biogeography illustrates palaeoclimate change in the Late Cretaceous Indian Ocean. Cretaceous Research 23, 537–634.

Lees, J.A., 2007. New and rarely reported calcareous nannofossils from the Late Cretaceous of coastal Tanzania: outcrop samples and Tanzania Drilling Project Sites 5, 9 and 15. Journal of Nannoplankton Research 29, 39–65.

Lees, J.A., Bown, P.R., 2005. Calcareous nannofossil biostratigraphy, ODP Leg 198 (Shatsky Rise, NW Pacific Ocean). Proceedings of the Ocean Drilling Program. Scientific Results 198, 1–60.

Li, L., Keller, G., 1998. Maastrichtian climate, productivity and faunal turnovers in planktic foraminifera in South Atlantic DSDP Sites 525A and 21. Marine Micropaleontology 33, 55–86.

Linares, D., 1977. Foraminíferos Planctónicos del Cretácico Superior de las Cordilleras Béticas (Sector Central). Publicaciones del Departamento de Geología, Universidad de Málaga, 410 pp.

Lirer, F., 2000. A new technique for retrieving calcareous microfossils from lithified lime deposits. Micropaleontology 46, 365–369.

MacLeod, K.G., Orr, W.N., 1993. The taphonomy of Maastrichtian inoceramids in the Basque Region of France and Spain and the pattern of their decline and disappearance. Paleobiology 19, 235–250.

MacLeod, N., Rawson, P.F., Forey, P.L., Banner, F.T., BouDagher–Fadel, M.K., Bown, P.R., Burnett, J.A., Chambers, P., Culver, S., Evans, S.E., Jeffery, C., Kaminski, M.A., Lord, A.R., Milner, A.C., Milner, A.R., Morris, N., Owen, E., Rosen, B.R., Smith, A.B., Taylor, P.D., Urquhart, E., Young, J.R., 1997. The Cretaceous–Tertiary biotic transition. Journal of the Geological Society, London 154, 265–292.

Mary, C., Moreau, M.G., Orue-Etxebarria, Apellaniz, E., Courtillot, V., 1991. Biostratigraphy and magnetostratigraphy of the Cretaceous/Tertiary Sopelana section (Basque Country). Earth and Planetary Science Letters 106, 133–150.

Mathey, B., 1982. El Cretácico del Arco Vasco. In: García, E. (Ed.), El Cretácico de España. Universidad Complutense de Madrid, pp. 111–135.

Melinte, M., Odin, G., 2001. Optical studies of the calcareous nannofossils from Tercis les Bains (Landes, SW France) at the Campanian–Maastrichtian Boundary. In: Odin, G.S. (Ed.), The Campanian–Maastrichtian Stage Boundary: Characterisation at Tercis les Bains (France) and Correlation with Europe and other Continents. Developments in Palaeontology and Stratigraphy, vol. 19. Elsevier, Amsterdam, pp. 285–292.

Molina, E., Alegret, L., Arenillas, I., Arz, J.A., Gallala, N., Grajales–Nishimura, M., Murillo–Muñetón, G., Zaghbib–Turki, D., 2009. The Global Boundary Stratotype Section and Point for the base of the Danian Stage (Paleocene, Paleogene, "Tertiary", Cenozoic): auxiliary sections and correlation. Episodes 32, 84–95.

Molina, E., Alegret, L., Arenillas, I., Arz, J.A., Gallala, N., Hardenbol, J., von Salis, K., Steurbaut, E., Vandenberghe, N., Zaghbib-Turki, D., 2006. The Global Stratotype Section and Point of the Danian Stage (Paleocene, Paleogene, "Tertiary", Cenozoic) at El Kef, Tunisia: original definition and revision. Episodes 29, 263–278.

Monechi, S., Thierstein, H.R., 1985. Late Cretaceous–Eocene nannofossil and magnetostratigraphic correlations near Gubbio, Italy. Marine Micropaleontology 9, 419–440.

Moreau, M.G., Cojan, I., Ory, J., 1994. Mechanisms of remanent magnetization in marl and limestone alternations. Case study: Upper Cretaceous (Chron 31–30), Sopelana, Basque Country. Earth and Planetary Science Letters 123, 15–37.

Mount, J.F., Ward, P., 1986. Origin of limestone/marl alternations in the upper Maastrichtian of Zumaya, Spain. Journal of Sedimentary Petrology 56, 228–236.

Mount, J.F., Margolis, S., Showers, W., Ward, P.D., Doehne, E., 1986. Carbon and oxygen isotope stratigraphy of the Upper Maastrichtian, Zumaya, Spain: a record of oceanographic and biologic changes at the end of the Cretaceous period. Palaios 1, 87–92.

Nederbragt, A.J., 1989. Chamber proliferation in the Cretaceous planktonic foraminifera Heterohelicidae. Journal of Foraminiferal Research 19, 105–114.

Nederbragt, A.J., 1990. Biostratigraphy and paleoceanographic potential of the Cretaceous planktic foraminifera Heterohelicidae. Academisch Proefschrift, Centrale Huisdrukkerij Vrije Universiteit, Amsterdam, 203 pp.

Nederbragt, A.J., 1991. Late Cretaceous biostratigraphy and development of Heterohelicidae (planktic foraminifera). Micropaleontology 37, 329–372.

Odin, G.S., 2001. Numerical age calibration of the Campanian–Maastrichtian succession at Tercis les Bains (Landes, France) and in the Bottaccione Gorge (Italy). In: Odin, G.S. (Ed.), The Campanian–Maastrichtian Stage Boundary: Characterisation at Tercis les Bains (France) and Correlation with Europe and other Continents. Developments in Palaeontology and Stratigraphy, vol. 19. Elsevier, Amsterdam, pp. 775–782.

Odin, G.S., Lamaurelle, M.A., 2001. The global Campanian/Maastrichtian stage boundary. Episodes 24, 229–238.

Odin, G.S., the Maastrichtian Working Group Members, 1996. Definition of a global Boundary Stratotype Section and Point for the Campanian/Maastrichtian boundary. Supplement. In: Rawson, P.F., D'Hondt, A.V., Hancock, J.M., Kennedy, W.J. (Eds.), Proceedings Second International Symposium on Cretaceous Boundaries, Brussels, 8–16 September, 1995. Bulletin de l'Institut Royal des Sciences Naturelles de Belgique, Sciences de la Terre, vol. 66, pp. 111–117.

Odin, G.S., the Maastrichtian Working Group Members, 2001a. The Campanian–Maastrichtian boundary: definition at Tercis (Landes, SW France) principle, procedure, and proposal. In: Odin, G.S. (Ed.), The Campanian–Maastrichtian Stage Boundary: Characterisation at Tercis les Bains (France) and Correlation with Europe and other Continents. Developments in Palaeontology and Stratigraphy, vol. 19. Elsevier, Amsterdam, pp. 820–833.

Odin, G.S., Arz, J.A., Caron, M., Ion, J., Molina, E., 2001b. Campanian–Maastrichtian planktonic foraminifera at Tercis les Bains (Landes, France); synthetic view and potential for global correlation. In: Odin, G.S. (Ed.), The Campanian–Maastrichtian Stage Boundary: Characterisation at Tercis les Bains (France) and Correlation with Europe and other Continents. Developments in Palaeontology and Stratigraphy, vol. 19. Elsevier, Amsterdam, pp. 379–395.

Ogg, J.G., Ogg, G., Gradstein, F.M., 2008. The Concise Geologic Time Scale. Cambridge University Press, Cambridge, 177 pp.

Paul, C.R.C., Lamolda, M.A., 2007. Carbon and oxygen stable isotopes in the Maastrichtian of the Basque Country, N. Spain. Cretaceous Research 28, 812–820.

Perch-Nielsen, K., 1985. Mesozoic calcareous nannofossils. In: Bolli, H.M., Saunders, J.B., Perch-Nielsen, K. (Eds.), Plankton Stratigraphy. Cambridge University Press, Cambridge, pp. 329–426.

Petrizzo, M.R., 2001. Late Cretaceous planktonic foraminifera from Kerguelen Plateau (ODP Leg 183): new data to improve the Southern Ocean biozonation. Cretaceous Research 22, 829–855.

Premoli Silva, I., Sliter, W.V., 1995. Cretaceous planktonic foraminiferal biostratigraphy and evolutionary trends from the Bottaccione section, Gubbio, Italy. Paleontographia Italica 82, 1–89.

Robaszynski, F., Caron, M., 1995. Foraminifères planctoniques du Crétacé: commentaire de la zonation Europe–Méditerranée. Bulletin de la Société Géologique de France 166, 681–692.

Robaszynski, F., Caron, M., González-Donoso, J.M., Wonders, A.A.H., the European Working Group on Planktonic Foraminifera, 1984. Atlas of Late Cretaceous Globotruncanids. Revue de Micropaléontologie 26, 145–305.

Robaszynski, F., Mzoughi, M., 2010. The Abiod at Ellès (Tunisia): stratigraphies, Campanian–Maastrichtian boundary, correlation with Kalaat Senan and the Tercis (France) stratotype. Carnets de Géologie/Notebooks on Geology. Article 2010/04 (CG2010_A04).

Robaszynski, F., González-Donoso, J.M., Linares, D., Amédro, F., Caron, M., Dupuis, C., d'Hondt, A.V., Gartner, S., 2000. Le Crétacé supérieur de la region de Kalaat Senan, Tunisie Centrale. Litho-biostratigraphie intégrée: zones d'ammonites, de foraminifers planctoniques et de nannofossiles du Turonien supérieur au Maastrichtien. Bulletin des Centres de Recherche et d'Exploration-Production, Elf-Aquitaine 22, 359–490.

Schulte, P., Alegret, L., Arenillas, I., Arz, J.A., Barton, P.J., Bown, P.R., Bralower, T.J., Christeson, G.L., Claeys, P., Cockell, C.S., Collins, G.S., Deutsch, A., Goldin, T.J., Goto, K., Grajales-Nishimura, J.M., Grieve, R.A.F., Gulick, S.P.S., Johnson, K.R., Kiessling, W., Koeberl, C., Kring, D.A., MacLeod, K.G., Matsui, T., Melosh, J., Montanari, A., Morgan, J.V., Neal, C.R., Nichols, D.J., Norris, R.D., Pierazzo, E., Ravizza, G., Rebolledo-Vieyra, M., Reimold, W.U., Robin, E., Salge, T., Speijer, R.P., Sweet, A.R., Urrutia-Fucugauchi, J., Vajda, V., Whalen, M.T., Willumsen, P.S., 2010. The Chicxulub asteroid impact and mass extinction at the Cretaceous–Paleogene boundary. Science 327, 1214–1218.

Schwentke, W., Kuhnt, W., 1992. Subsidence history and continental margin evolution of the Western Pyrenean and Basque basins. Palaeogeography, Palaeoclimatology, Palaeoecology 95, 297–318.

Sheldon, E., 2008. Upper Campanian–Maastrichtian calcareous nannofossil biostratigraphy of the Stevns-1 borehole, Denmark. Journal of Nannoplankton Research 30, 39–49.

Sissingh, W., 1977. Biostratigraphy of Cretaceous calcareous nannoplankton. Geologie en Mijnbouw 57, 433–440.

Smith, C.C., Pessagno, E.A., 1973. Planktonic foraminifera and stratigraphy of the Corsicana Formation (Maastrichtian), north-central Texas. In: Cushman Foundation for Foraminiferal Research, Special Publication, vol. 112. 1–68.

ten Kate, W.G.H.Z., Sprenger, A., 1993. Orbital cyclicities above and below the Cretaceous/Paleogene boundary at Zumaya (N Spain), Agost and Relleu (SE Spain). Sedimentary Geology 87, 69–101.

Thibault, N.R., 2010. Calcareous nannofossils from the Boreal upper Campanian–Maastrichtian Chalk of Denmark. Journal of Nannoplankton Research 31, 39–56.

von Salis, K., 2001. Calcareous nannofossils around the Campanian/Maastrichtian Boundary at Tercis, France. In: Odin, G.S. (Ed.), The Campanian–Maastrichtian Stage Boundary: Characterisation at Tercis les Bains (France) and Correlation

with Europe and other Continents. Developments in Palaeontology and Stratigraphy, vol. 19. Elsevier, Amsterdam, pp. 268–271.
Wagreich, M., Küchler, T., Summesberger, H., 1998. Integrated nannofossil, planktonic foraminifera and ammonite stratigraphy of some European key sections: Santonian–Campanian and Campanian–Maastrichtian boundaries. Abstracts of the 16th Congress of the Carpathian–Balkan Geological Association, Vienna, p. 632.
Wagreich, M., Küchler, T., Summesberger, H., 2003. Correlation of calcareous nannofossil zones to the local first occurrence of *Pachydiscus neubergicus* (von Hauer, 1858) (Ammonoidea) in European Upper Cretaceous sections. Geologie en Mijnbouw 82, 283–288.
Ward, P.D., 1988. Maastrichtian ammonite and inoceramid ranges from Bay of Biscay Cretaceous–Tertiary boundary sections. In: Lamolda, M.A., Kauffman, E.G., Walliser, O.H. (Eds.), Paleontology and Evolution: Extinction Events. Revista Española de Paleontología, No. Extraordinario, pp. 119–126.
Ward, P.D., Kennedy, W.J., 1993. Maastrichtian ammonites from the Biscay Region (France, Spain). Journal of Paleontology, Memoir 34, 1–58.
Ward, P.D., Kennedy, W.J., MacLeod, K.G., Mount, J.F., 1991. Ammonite and inoceramid bivalve extinction patterns in Cretaceous/Tertiary boundary sections of the Biscay region (southwestern France, northern Spain). Geology 19, 1181–1184.
Watkins, D.K., Wise S.W., Jr., Pospichal, J.J., Crux, J., 1996. Upper Cretaceous calcareous nannofossil biostratigraphy and paleoceanography of the Southern Ocean. In: Moguilevsky, A., Whatley, R. (Eds.), Microfossils and Oceanic Environments. University of Wales, Aberystwyth Press, pp. 355–381.
Wiedmann, J., 1988. The Basque coastal sections of the K/T boundary – a key to understanding "mass extinctions" in the fossil record. No. Extraordinario. In: Lamolda, M.A., Kauffman, E.G., Walliser, O.H. (Eds.), Paleontology and Evolution: Extinction Events. Revista Española de Paleontología, pp. 127–140.

Appendix

Taxonomic list of planktonic foraminifera
Abathomphalus intermedius (Bolli, 1951)
Abathomphalus mayaroensis (Bolli, 1951)
Archaeoglobigerina blowi Pessagno, 1967
Archaeoglobigerina cretacea (d'Orbigny, 1840)
Contusotruncana contusa (Cushman, 1926)
Contusotruncana fornicata (Plummer, 1931)
Contusotruncana morozovae (Vasilenko, 1961)
Contusotruncana patelliformis (Gandolfi, 1955)
Contusotruncana plicata (White, 1928)
Contusotruncana plummerae (Gandolfi, 1955)
Contusotruncana walfischensis (Todd, 1970)
Globigerinelloides multispina (Lalicker, 1948)
Globigerinelloides prairiehillensis (Pessagno, 1967)
Globigerinelloides rosebudensis Smith and Pessagno, 1973
Globigerinelloides subcarinatus (Brönnimann, 1952)
Globigerinelloides volutus (White, 1928)
Globigerinelloides yaucoensis (Pessagno, 1960)
Globotruncana aegyptiaca Nakkady, 1950
Globotruncana arca (Cushman, 1926)
Globotruncana bulloides Vogler, 1941
Globotruncana falsostuarti Sigal, 1952
Globotruncana linneiana (d'Orbigny, 1839)
Globotruncana mariei Banner and Blow, 1960
Globotruncana orientalis El Naggar, 1966
Globotruncana rosetta (Carsey, 1926)
Globotruncana ventricosa White, 1928
Globotruncanella havanensis (Voorwijk, 1937)
Globotruncanella minuta Caron and González Donoso, 1984
Globotruncanella petaloidea (Gandolfi, 1955)
Globotruncanita angulata (Tilev, 1951)
Globotruncanita conica (White, 1928)
Globotruncanita dupeublei (Caron, González Donoso, Robaszynski and Wonders, 1984)
Globotruncanita fareedi (El Naggar, 1966)
Globotruncanita insignis (Gandolfi, 1955)
Globotruncanita stuarti (de Lapparent, 1918)
Globotruncanita stuartiformis (Dalbiez, 1955)
Gublerina acuta de Klasz, 1953
Gublerina cuvillieri Kikoine, 1948
Guembelitria cretacea Cushman, 1933
Hedbergella holmdelensis Olsson, 1964
Hedbergella monmouthensis (Olsson, 1960)
Heterohelix glabrans (Cushman, 1938)
Heterohelix globulosa (Ehrenberg, 1840)
Heterohelix labellosa Nederbragt, 1991
Heterohelix navarroensis (Loeblich, 1951)
Heterohelix planata (Cushman, 1938)
Heterohelix pulchra (Brotzen, 1936)
Heterohelix punctulata (Cushman, 1938)
Planoglobulina acervulinoides (Egger, 1899)
Planoglobulina carseyae (Plummer, 1931)
Planoglobulina manuelensis (Martin, 1972)
Planoglobulina multicamerata (de Klasz, 1953)
Planoglobulina riograndensis (Martin, 1972)
Pseudoguembelina costellifera Masters, 1976
Pseudoguembelina costulata (Cushman, 1938)
Pseudoguembelina excolata (Cushman, 1926)
Pseudoguembelina hariaensis Nederbragt, 1991
Pseudoguembelina kempensis Esker, 1968
Pseudoguembelina palpebra Brönnimann and Brown, 1953
Pseudotextularia elegans (Rzehak, 1891)
Pseudotextularia intermedia de Klasz, 1953
Pseudotextularia nuttalli (Voorwijk, 1937)
Racemiguembelina fructicosa (Egger, 1899)
Racemiguembelina powelli (Smith and Pessagno, 1973)
Rugoglobigerina hexacamerata Brönnimann, 1952
Rugoglobigerina macrocephala Brönnimann, 1952
Rugoglobigerina milamensis Smith and Pessagno, 1973
Rugoglobigerina pennyi Brönnimann, 1952
Rugoglobigerina rotundata Brönnimann, 1952
Rugoglobigerina rugosa (Plumier, 1926)
Rugoglobigerina scotti (Brönnimann, 1952)